

EFFECT OF STABILIZER ON THE CATALYTIC ACTIVITY OF COBALT(0)
NANOCLUSTERS CATALYST IN THE HYDROLYSIS OF SODIUM
BOROHYDRIDE

A THESIS SUBMITTED TO
THE GRADUATE SCHOOL OF NATURAL AND APPLIED SCIENCES
OF
MIDDLE EAST TECHNICAL UNIVERSITY

BY

EBRU KOÇAK

IN PARTIAL FULFILLMENT OF THE REQUIREMENTS
FOR
THE DEGREE OF MASTER OF SCIENCE
IN
CHEMISTRY

DECEMBER 2009

Approval of the thesis:

**EFFECT OF STABILIZER ON THE CATALYTIC ACTIVITY OF
COBALT(0) NANOCCLUSERS CATALYST IN THE HYDROLYSIS OF
SODIUM BOROHYDRIDE**

submitted by **EBRU KOÇAK** in partial fulfillment of the requirements for the degree of **Master of Science in Chemistry Department, Middle East Technical University** by,

Prof. Dr. Canan Özgen
Dean, Graduate School of **Natural and Applied Sciences**

Prof. Dr. Ahmet M. Önal
Head of Department, **Chemistry**

Prof. Dr. Saim Özkar
Supervisor, **Chemistry Dept., METU**

Examining Committee Members:

Prof. Dr. Zuhâl Küçükyavuz
Chemistry Dept., METU

Prof. Dr. Saim Özkar
Chemistry Dept., METU

Prof. Dr. Ceyhan Kayran
Chemistry Dept., METU

Prof. Dr. Birgöl Karan
Chemistry Dept., Hacettepe University

Assoc. Prof. Dr. Ayşen Yılmaz
Chemistry Dept., METU

Date: December 18, 2009

I hereby declare that all information in this document has been obtained and presented in accordance with academic rules and ethical conduct. I also declare that, as required by these rules and conduct, I have fully cited and referenced all material and results that are not original to this work.

Name, Last name : Ebru KOÇAK

Signature :

ABSTRACT

EFFECT OF STABILIZER ON THE CATALYTIC ACTIVITY OF COBALT(0) NANOCLUSTERS CATALYST IN THE HYDROLYSIS OF SODIUM BOROHYDRIDE

Koçak, Ebru

M.S., Department of Chemistry

Supervisor: Prof. Dr. Saim Özkar

December 2009, 64 pages

The development of new storage materials will facilitate the use of hydrogen as a major energy carrier in near future. Among the chemical hydrides used as hydrogen storage materials for supplying hydrogen at ambient temperature, sodium borohydride seems to be an ideal one because it is stable under ordinary conditions and liberates hydrogen gas in a safe and controllable way in aqueous solutions. However, self hydrolysis of sodium borohydride is so slow that requires a suitable catalyst. This work aims the use of water dispersible cobalt(0) nanoclusters having large portion of atoms on the surface as catalyst for the hydrolysis of sodium borohydride. In-situ formation of cobalt(0) nanoclusters and catalytic hydrolysis of sodium borohydride were performed starting with a cobalt(II) chloride as precursor and sodium borohydride as reducing agent and substrate in the presence of a water soluble stabilizer. As stabilizer, water soluble polyacrylic acid as well as hydrogen

phosphate ion were tested. Cobalt(0) nanoclusters were characterized by using all the available analytical methods including FT-IR, TEM, XPS, UV-visible electronic absorption spectroscopy. The kinetics of cobalt(0) nanoclusters catalyzed hydrolysis of sodium borohydride were studied depending on the catalyst concentration, substrate concentration, stabilizing agent concentration and temperature.

Keywords: Cobalt(0) nanoclusters, hydrolysis of sodium borohydride, heterogeneous catalyst, homogeneous catalyst, hydrogenphosphate, polyacrylic acid, TEM, XPS, FT-IR, UV-Vis

ÖZ

SODYUM BORHİDRÜRÜN HİDROLİZİ İÇİN KATALİZÖR OLARAK KULLANILAN KOBALT(0) NANOKÜMELERİNİN KATALİTİK AKTİVİTESİNE KARARLAŞTIRICININ ETKİSİ

Koçak, Ebru

Yüksek Lisans, Kimya Bölümü

Tez Yöneticisi: Prof. Dr. Saim Özkar

Aralık 2009, 64 sayfa

Yeni hidrojen depolama malzemelerindeki gelişim hidrojenin temel enerji taşıyıcısı olarak yakın gelecekte kullanımını hızlandıracaktır. Hidrojen depolama malzemesi olarak kullanılan kimyasal hidrürler arasında sodyum borhidrür, kararlı, güvenli ve sulu çözeltilerde kontrol edilebilir olması nedeniyle en ideal olanıdır. Ancak sodyum borhidrürün hidrolizi çok yavaş olduğundan uygun bir katalizör kullanımını gerektirmektedir. Bu çalışmanın amacı, atomlarının büyük bir kısmını yüzeyde tutan kobalt(0) nanokümlerinin, sodyum borhidrürün hidrolizinde katalizör olarak kullanımınıdır. Kobalt(0) nanokümlerinin yerinde oluşumu ve sodyum borhidrürün katalitik hidrolizi, kobalt(II) klorür tuzunun başlangıç maddesi olarak ve sodyum borhidrürün suda çözünebilir bir kararlaştırıcı varlığında substrat ve indirgen olarak kullanımıyla gerçekleştirildi. Kararlaştırıcı olarak hidrojenfosfat iyonu gibi suda çözülebilen bir polimer olan poliakrilik asit de denendi. Kobalt(0) nanokümlerini tanımlanması FT-IR, TEM, XPS, UV-Görünür elektronik

absorpsiyon spektroskopisi kullanılarak yapıldı. Sodyum borhidrürün hidrolizinde katalizör olarak kullanılan kobalt(0) nanokümelerinin kinetik çalışması katalizör derişimi, substrat derişimi kararlaştırıcı derişim ve sıcaklığa bağı olarak çalışıldı.

Anahtar Kelimeler: Kobalt(0) nanokümeleri; Sodyum borhidrürün hidrolizi; heterojen katalizör, homojen katalizör, hidrojenfrosfat, poliakrilik asit, TEM, XPS, FT-IR, UV-Görünür Spektrokopisi.

To My Family...

ACKNOWLEDGEMENTS

I would like to express my sincere gratitude to Prof. Dr. Saim Özkar for his great support, supervision and understanding throughout in this study.

I wish to express my sincere appreciation to Önder Metin for his support and guidance during my study.

I would like to thank my lab partners, Mehmet, Dilek, Murat, Ebru, Huriye, Serdar, Tuğçe and Salim for their caring, never ending helps and their encouragement during my study.

I would like to thank Balam Balık for her friendship, support, understanding, and encouragement throughout in this challenging period.

I would like to thank Beyza, Hava, İlker, Abdullah and Şüheda for making everything much more easier for me. Thank you all for being there whenever I need.

I also express my thanks to Chemistry Department of Middle East Technical University for providing facilities used in this study.

The last but not least, I would like to extend my gratitude to my family for helping me with every problem I encountered during the whole study.

TABLE OF CONTENTS

ABSTRACT.....	iv
ÖZ.....	vi
ACKNOWLEDGEMENTS.....	ix
TABLE OF CONTENTS.....	x
LIST OF TABLES.....	xiii
LIST OF FIGURES.....	xiv
CHAPTERS	
1 INTRODUCTION.....	1
2 HYDROGEN ECONOMY	5
2.1 Global Energy Problems.....	5
2.2 Hydrogen as an Energy Carrier.....	6
2.3 Sodium Borohyride as a Hydrogen Storage Material.....	7
3 TRANSITION METAL NANOCLUSTERS.....	10
3.1 Colloidal Metal Nanoclusters.....	10
3.2 Stabilization of Metal Nanoparticles	11
3.2.1 Electrostatic Stabilization	11
3.2.2 Steric Stabilization	12
3.3 Preparation of Metal Nanoparticles.....	13
3.3.1 Chemical Reduction of Transition Metal Salts.....	13
3.3.2 Reduction by Electrochemical Methods.....	14
3.3.3 Displacements of Ligands from Organometallic Complexes.....	14
3.4 Characterization of Metal Nanoparticles.....	14
4 EXPERIMENTAL.....	16
4.1. Materials.....	16
4.2. In-situ Formation of Hydrogenphosphate-stabilized Cobalt(0) Nanoclusters and Catalytic Hydrolysis of Sodium	

Borohydride.....	16
4.3. In-situ Formation of Poly(acrylic acid)-stabilized Cobalt(0) Nanoclusters and Catalytic Hydrolysis of Sodium Borohydride	17
4.4. Self Hydrolysis Of Sodium Borohydride.....	19
4.5. Kinetic Study Of Hydrogenphosphate-Stabilized Cobalt(0) Nanocluster In Catalytic Hydrolysis Of Sodium Borohydride.....	19
4.6. Kinetic Study Of Poly(acrylic acid) -Stabilized Cobalt(0) Nanocluster In Catalytic Hydrolysis Of Sodium Borohydride.....	20
4.7. Effect Of Hydrogenphosphate Concentration On The Catalytic Activity Of Cobalt(0) Nanoclusters.....	20
4.8. Effect Of Poly(acrylic acid) Concentration On The Catalytic Activity Of Cobalt(0) Nanoclusters	21
4.9. Catalytic Lifetime Of Hydrogenphosphate-Stabilized and Poly(acrylic acid)-Stabilized Cobalt(0) Nanoclusters	21
4.10. Characterization of Hydrogenphosphate-Stabilized and Poly(acrylic acid)-Stabilized Cobalt(0) Nanoclusters.....	22
4.10.1. TEM Analysis.....	22
4.10.2. XPS (X-Ray photoelectron spectroscopy).....	22
4.10.3. FT-IR Spectra.....	23
4.10.4. UV-vis Study.....	23
5 RESULTS AND DISCUSSION.....	25
5.1. In-Situ Formation of Hydrogen Phosphate-stabilized and Poly(acrylic acid)-stabilized Cobalt(0) Nanoclusters and Catalytic Hydrolysis of Sodium Borohydride.....	25
5.2. Effect of Hydrogen Phosphate and Poly(acrylic acid) Concentration on the Stability and Activity of Cobalt(0) Nanoclusters Catalyst.....	29
5.3. Reduction of Cobalt(II) Chloride by Sodium Borohydride.....	32
5.4. Integrity of Stabilizers.....	34

5.5. Lifetime of Catalyst.....	36
5.6. Kinetics of Hydrolysis of Sodium Borohydride catalyzed by Hydrogen Phosphate-stabilized and Poly(acrylic acid)-stabilized Cobalt(0) Nanoclusters.....	37
6 CONCLUSIONS.....	51
REFERENCES.....	54
APPENDIX A	59

LIST OF TABLES

TABLES

Table 5.1. Rate constants for the hydrolysis of sodium borohydride catalyzed by Co(0) nanoclusters starting with a solution of 150 mM NaBH ₄ and 1.4 mM Cobalt(0) nanoclusters at different temperatures in the presence of hydrogen phosphate as stabilizer	43
Table 5.2. Rate constants for the hydrolysis of sodium borohydride catalyzed by Co(0) nanoclusters starting with a solution of 150 mM NaBH ₄ and 1.4 mM Cobalt(0) nanoclusters at different temperatures in the presence of poly(acrylic acid) as stabilizer.	46
Table 5.3. Arrhenius activation energy for various catalyst systems used for the hydrolysis of sodium borohydride.....	48

LIST OF FIGURES

FIGURES

Figure 2.1. Volumetric hydrogen density versus gravimetric hydrogen density of various hydrogen containing compounds.....	8
Figure 3.1. Schematic representation of electrostatic stabilization.....	12
Fig.3.2. Schematic representation of steric stabilization	12
Figure 3.3. Common methods available for nanoparticles characterization	15
Figure 4.1. The experimental setup used in performing the catalytic hydrolysis of sodium borohydride and measuring the hydrogen generation rate.....	18
Figure 5.1. UV-visible spectra of hydrogen phosphate stabilized Co(0) nanoclusters.....	26
Figure 5.2. UV-visible spectra of poly(acrylic acid) stabilized Co(0) nanoclusters..	27
Figure 5.3. (a) TEM image and (b) associated histogram of hydrogen phosphate stabilized cobalt(0) nanoclusters	28
Figure 5.4. (a) TEM image and (b) associated histogram of poly(acrylic acid) stabilized cobalt(0) nanoclusters	28
Figure 5.5. The graph of volume of hydrogen versus time for the hydrolysis of sodium borohydride catalyzed by hydrogen phosphate-stabilized cobalt(0) nanoclusters starting with various hydrogenphosphate concentrations at 25 ± 0.1 °C. $[\text{Co}] = 1.4$ mM, $[\text{NaBH}_4] = 150$ mM	29
Figure5. 6. Hydrogen generation rate versus $[\text{HPO}_4]/[\text{Co}]$ ratio at 25.0 ± 0.1 °C	30
Figure 5.7. The graph of volume of hydrogen versus time for the hydrolysis of sodium borohydride catalyzed by cobalt(0) nanoclusters starting with various poly(acrylic acid) concentrations at 25 ± 0.1 °C. $[\text{Co}] =$	

1.4 mM, [NaBH ₄] =150mM.....	31
Figure 5. 8. Hydrogen generation rate versus [PAA]/[Co] ratio at 25.0 ± 0.1 °C	32
Figure 5.9. XPS spectrum of hydrogenphosphate-stabilized cobalt(0) nanocluster.	33
Figure 5.10. XPS spectrum of poly(acrylic acid)-stabilized cobalt(0) nanoclusters..	34
Figure 5.11. FT-IR Spectra of hydrogen phosphate-stabilized Co(0) nanoclusters...	35
Figure 5.12. FT-IR Spectra of poly(acrylic acid)-stabilized Co(0) nanoclusters.....	36
Fig. 5.13. The graph of volume of hydrogen (mL) versus Time (s) in different Co(II) chloride concentrations in all sets [NaBH ₄] = 150 mM where in the presence of hydrogen phosphate as stabilizer	38
Fig. 5.14. The graph of volume of hydrogen (mL) versus Time (s) in different Co(II) chloride concentrations in all sets [NaBH ₄] = 150 mM where in the presence of poly(acrylic acid) as stabilizer	39
Fig. 5.15. The graph of ln Rate versus ln [Co] at 25 oC and 150 mM NaBH ₄ in the presence of hydrogenphosphate-stabilizer	40
Fig. 5.16. The graph of ln Rate versus ln [Co] at 25 oC and 150 mM NaBH ₄ in the presence of poly(acrylic acid)-stabilizer	40
Fig. 5.17. The graph of ln rate versus ln [NaBH ₄] at constant [Co]=1.4 mM in the presence of hydrogen phosphate-stabilizer	41
Fig. 5.18. The graph of ln rate versus ln [NaBH ₄] at constant [Co]=1.4 mM in the presence of poly(acrylic acid)-stabilizer	42
Figure 5.19. The grafph of Time(s) vs Volume of hydrogen in different temperature In all sets [Co]=1.4mM, [NaBH ₄]=150mM and [HPO ₄ 2-]=4.2mM	43
Figure 5.20. The Arrhenius plot, lnk versus the reciprocal absolute temperature 1/T, for the hydrolysis of sodium borohydride catalyzed by hydrogenphosphate stabilized cobalt(0) nanoclusters in the temperature range is 25- 45 °C.....	45
Figure 5.21. The grafph of Time(s) vs Volume of hydrogen in different temperature In all sets [Co]=1.4mM, [NaBH ₄]=150mM and [PAA]=4.2mM.....	46

Figure 5.22. The Arrhenius plot, $\ln k$ versus the reciprocal absolute temperature $1/T$, for the hydrolysis of sodium borohydride catalyzed by poly(acrylic acid)-stabilized cobalt(0) nanoclusters in the temperature range is 20- 40 oC.	47
Figure 5.23. The Eyring plot, $\ln (k/T)$ versus the reciprocal absolute temperature $1/T$, for the hydrolysis of sodium borohydride catalyzed by hydrogenphosphate-stabilized cobalt(0) nanoclusters in the temperature range 25-45 oC.....	49
Figure 5.24. The Eyring plot, $\ln (k/T)$ versus the reciprocal absolute temperature $1/T$, for the hydrolysis of sodium borohydride catalyzed by poly(acrylic acid)-stabilized cobalt(0) nanoclusters in the temperature range 20-40 oC.....	50

CHAPTER 1

INTRODUCTION

World's primary energy sources (fossil fuels) meet the 80 % of the energy demand today [1]. However, use of fossil fuels as primary energy sources causes serious environmental problems [2]. Additionally, fossil fuels are not renewable energy sources and so it is expected that the fossil fuel reserves will be destined to run out in future [3]. Therefore, there is an urgent need to find alternative, clean and renewable energy sources such as wind energy, solar energy, hydropower, and biomass energy. However, renewable energy sources have some drawbacks such as discontinuity between energy sources and demand (sun does not shine and wind does not blow everytime) [4]. In this regard, storage of energy is very important issue. Hydrogen is not a primary energy source but it can be used as an energy carrier due to the lots of advantages such as it has an abundant and secure source, clean, renewable, and widely available from diverse sources [5]. Using hydrogen as an energy carrier has many advantages and seems to have a key role to solve the future energy problems [6]. Hydrogen economy deals with three basic research area; 1) Hydrogen production: to find different sources to produce hydrogen, 2) Hydrogen storage: finding an efficient way to store hydrogen, 3) Fuel-cells: reducing the cost of the fuel-cells. Hydrogen can be produced from numerous sources [7] however, storage and use of hydrogen are still being problem due to the its very low density for on-board usage which must be studied to increase the efficiency and to decrease the cost [8]. Up to now, many chemical hydrides have been tested for hydrogen storage materials, and a few of them appear to be promising to store hydrogen. Among the chemical hydrides sodium borohydride, NaBH_4 , is most valuable material for hydrogen storage due to the lots of advantages such as stability in solid state, having high hydrogen content (10.8 wt%), nonflammability, ease of handling

and non-toxicity. of hydrogen [9]. Sodium borohydride reacts with water, which is called hydrolysis, to generate hydrogen and water-soluble sodium metaborate, NaBO₂, at ambient temperature (**Eq.1**) [10].



The practical use of equation 1 requires a suitable catalyst to achieve ambient hydrogen generation rate [11]. Up to know, different catalysts were tested for the hydrolysis of NaBH₄: platinum or rhodium salts [12], cobalt salt [13], iron, ruthenium, palladium, osmium, iridium, and platinum salts [14], nickel, Raney nickel, and bulk cobalt [15], alloys such as LaNi_{4.5}T_{0.5} (T = Mn, Cr, Co, Fe, Cu) [16], bulk ruthenium [17], mixed metal/metal oxides such as Pt–LiCoO₂ [18], nickel boride [19] and filamentary nickel–cobalt [20]. With the exception of metal salts of platinum, ruthenium [12] and cobalt [13], all of the catalysts used for the hydrolysis of sodium borohydride were heterogeneous [21]. The activity of heterogeneous catalysts is directly related to surface area, and so classical heterogeneous catalysts have limited surface area with the lower catalytic activity. Decreasing particle size of the heterogeneous catalyst is very promising way to increase the catalytic activity. In this scenario, transition metal nanoclusters having particle size 1-10 nm with large surface area can be used as highly active catalyst [22]. However, for the practical use of transition-metal nanoclusters as catalyst in solution, they must be stabilized against the agglomeration to bulk metal [23] because transition-metal nanoclusters are thermodynamically unstable due to having very large surface area relative to their masses which makes them having an excess surface free energy comparable to the lattice energy. Protective agents are therefore essential in order to be able to outweigh the attractive van der Waals forces by the repulsive electrostatic and steric forces between adsorbed ions and associated counterions. Depending on protecting shell type, there are mainly two stabilization methods: electrostatic and steric [24]. In electrostatic stabilization method, metallic particle surface interacts with electrical double layer formed by the anions and cations which concludes in electrostatic repulsion between particles [25]. On the

other hand, steric stabilization can be achieved by large organic molecules like polymers which are adsorbed on the surface of the nanoparticle form a protective layer [26]. In this study, cobalt(0) nanoclusters were synthesized for the first time by using both an electrostatic (hydrogenphosphate ion) and a steric stabilizer (poly(acrylic acid)).

In the light of explanations given so far, cobalt(0) nanoclusters stabilized in solution by a suitable stabilizer (electrostatic or steric) are thought to be a highly active catalyst for the hydrolysis of sodium borohydride. In this study, hydrogen phosphate and poly(acrylic acid) used as stabilizer for the synthesis of cobalt(0) nanoclusters in-situ during the hydrolysis of sodium borohydride in aqueous solution. HPO_4^{2-} ion has been predicted as a suitable electrostatic stabilizer for the cobalt(0) nanoclusters since it has O-O distance perfectly matching to the metal-metal distance of ca. 2.50 \AA in the cobalt(0) nanoclusters by lattice size-matching model [27]. Hydrogen phosphate ion has been shown to be a very good stabilizer for the nickel(0) [28] and iridium(0) [29] nanoclusters. Moreover, hydrogen phosphate is a water-soluble inorganic anion that can be chosen as stabilizer for the water-dispersible cobalt(0) nanoclusters for the hydrolysis of sodium borohydride. On the other hand, poly(acrylic acid) as a steric stabilizer was chosen among many of polymers such as polyvinylpyrrolidone, poly(4-styrene sulfonic acid-co-maleic acid), poly(2-ethyl-2-oxazoline), poly(ethylene glycol), poly(diallyldimethyl ammonium chloride) due to the best stability and catalytic activity of cobalt(0) nanoclusters. Thus hydrogen phosphate ion and poly(acrylic acid) were chosen as stabilizer for water dispersible cobalt(0) nanoclusters. The catalytic activity and stability of cobalt(0) nanoclusters were studied depending on the stabilizer concentration to find optimum stabilizer/metal ratio for both type of stabilizer. The kinetics of the hydrolysis of the sodium borohydride catalyzed by the both hydrogen phosphate and poly(acrylic acid) stabilized cobalt(0) nanoclusters were also studied depending on the catalyst concentration, substrate concentration and different temperatures. The reaction order, activation energy and activation parameters of catalytic hydrolysis reactions were found in the light of kinetic data for hydrogenphosphate-stabilized

cobalt(0) nanoclusters and poly(acrylic acid)-stabilized cobalt(0) nanoclusters catalyzed hydrolysis of sodium borohydride.

In addition to investigation kinetics of hydrogen generation from catalytic hydrolysis of sodium borohydride catalyzed by cobalt(0) nanoclusters, this study also provides a fundamental understanding of the effect of stabilizer type on the stability, catalytic activity, and lifetime of cobalt(0) nanoclusters as catalyst in the hydrolysis of sodium borohydride in aqueous media. Using two type of stabilizers will help to understand the basic influences of steric and electrostatic stabilizers on the catalytic activity by giving a chance to observe their influence on the same catalyst.

CHAPTER 2

HYDROGEN ECONOMY

2.1. Global Energy Problems

Energy has been one of the most important topics for the humankind since it is directly related to the civilization. From the existence of human beings, progress in economic and social development was supported by the various and effective energy options. Nations which give more attention to energy production than the others showed a significant improvement in their social and economical life [30].

Today, global energy is dominated by fossil fuels (85% of world consumption) which are destined to run out since they are limited sources on earth. Using fossil fuels as primary energy sources has many drawbacks for the environment like global climate change from carbon dioxide and methane emissions, air pollution problems, greenhouse gas emissions, etc. whereas energy demand is still increasing in all countries [31].

In today's world, nearly 29 billion tonnes of CO₂ are released into the air annually by human activities, including 23 billion from fossil fuel burning and industry according to the report of Intergovernmental Panel on Climate Change at 2001. Therefore, a quick and disturbing increase in the amount of CO₂ in the atmosphere occurs. For the limitation of releasing greenhouse gasses The United Nations Convention on Climate Change Protocol was signed in 1992, followed by the Kyoto conference in 1997. However, these international limitations are not enough as thinking the geopolitical and economic implications. World needs a new

and clean energy that will meet the increasing energy demand, will not threaten the nature and can be renewable for the sustainability [32].

2.2. Hydrogen as an Energy Carrier

Hydrogen is the ninth most common element in the universe. However, it does not exist in its pure form on earth. It is present in very large amounts combined with oxygen as water and combined with carbon and other elements in fossil fuels and lots of hydrocarbon compounds. Hydrogen is first isolated in 1766 by Henry Cavendish and after that time fuel-cell developments have started by the year 1839 and it is still being studied by researchers [33]. Since pure hydrogen does not exist on earth it is necessary to extract hydrogen from either water or hydrocarbons, both of which are abundant on earth.

Production of hydrogen must be developed well for a successful transition to the hydrogen economy so that the technology can be accomplished in a sustainable, clean, and economical manner not forgetting the fact that hydrogen is an energy carrier, not an energy source, and thus requires primary energy for its production. Today's hydrogen production is mainly based on biological processes, electrochemical water electrolysis, or chemical methods [34]. Considering the biological systems' low conversion efficiencies and the high cost of water electrolysis, hydrogen production is dominated by chemical methods [35]. Hydrogen can be chemically extracted from its sources by steam or partial oxidation reforming of natural gas, coal gasification by which approximately 95% hydrogen is generated at present [36]. However, raw materials used in these techniques are based on fossil fuels which are not clean and also not sustainable. The only advantage is their low cost but considering a stable solution, this will not be sufficient. On the other hand, reforming of biomass, water photolysis are the high cost techniques for the hydrogen production [37], [33].

Hydrogen storage is another important constituent for the development of the hydrogen economy. High-pressure compression and low-temperature liquefaction are

the basic techniques to store hydrogen today but these two techniques still need to improve to store hydrogen safely and to overcome technological problems. Whereas, using chemical hydrides for the hydrogen storage gives opportunity to store hydrogen safely [38]. NH_3 , $\text{NH}_2\text{-NH}_2$, $\text{NH}_3\text{-BH}_3$, LiH , NaAlH_4 , NaH and sodium borohydride (NaBH_4) are some of the chemical hydrides used for the hydrogen storage [39].

Production, storage and distribution of hydrogen is very important, if hydrogen will be the future's energy carrier. Studies are still continuing for the improvement of these issues.

2.3. Sodium Borohydride as a Hydrogen Storage Material

Hydrogen storage materials have crucial role for the development of future clean hydrogen energy system [40]. Hydrogen can be stored in different ways as explained before. Chemical hydrides play a key role for this application. Among the chemical hydrides sodium borohydride (NaBH_4) has an important place since it is stable, non-flammable and non-toxic in nature with hydrogen storing capability of 10,9 % by weight [39] shown in figure 2.1.

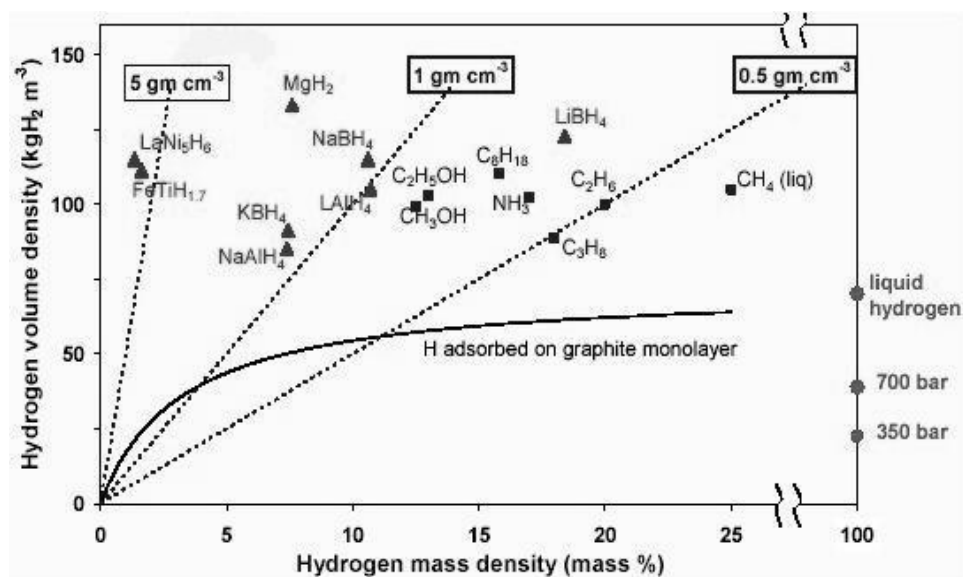


Figure 2.1. Volumetric hydrogen density versus gravimetric hydrogen density of various hydrogen containing compounds

A sodium borohydride solution is chemically stable in basic environment, not flammable, not explosive, and produces neither pollution nor by-products capable of causing the greenhouse effect. NaBH_4 appears as the only technology for storing hydrogen in liquid (aqueous) form [41].

Sodium borohydride hydrolyses according to the following exothermic reaction to produce water-soluble, environmentally benign sodium metaborate (NaBO_2) and hydrogen with the important advantage of producing half of the hydrogen from the water solvent [42]:



Reaction 1 occurs without a catalyst, if the solution $\text{pH} < 9$ [43]. Using a suitable catalyst will increase the efficiency of hydrogen production for this reaction [40], [39], [41], [42]. Many organic and inorganic acids are able to effectively enhance the hydrolysis reaction rate; however the reaction usually becomes

uncontrollable. On the other hand, solid state catalysts such as precious (generally functionalized with support) or transition metals and their salts are found to be very efficient in accelerating the hydrolysis reaction in a controllable manner [44].

This reaction is very efficient on a weight basis, since out of the 4 moles of H_2 that is produced, half comes from $NaBH_4$ and the other half from H_2O . And catalytic hydrogen production from $NaBH_4$ solutions also has many advantages [43]:

- Solutions of $NaBH_4$ are non-flammable
- Solutions of $NaBH_4$ are stable in air
- H_2 formation occurs in the presence of suitable catalyst
- Reaction products do not threaten the environment
- Rates of H_2 production can be controlled
- H_2 can be generated even at low temperatures
- H_2 efficiencies are high due to volumetric and gravimetric means

CHAPTER 3

TRANSITION METAL NANOCLUSTERS

3.1. Colloidal Metal Nanoclusters

Transition-metal nanoclusters, generally less than 10 nm (100 Å) in diameter, are in great interest since their effective applications in catalysis and holding the potential to serve as soluble analogues of heterogeneous catalysts in nanoparticle science [45], [46]. Quantum computers, photochemistry, optics, nanoelectronics, chemical sensors, etc. are other fields that nanoclusters can be applicable [47].

Nanostructured metal colloids can be prepared via two methods called “top down methods” and “bottom up methods”. Among these methods, “bottom up methods” are more applicable than “top down methods”. Chemical reduction of metal salts including electrochemical pathways, thermolysis including photolytic, radiolytic, and sonochemical pathways and controlled decomposition of pre-formed metastable organometallics are the methods for the preparation of wet chemical nanoparticles [48].

Nanoclusters can be used as catalyst in many reactions including spanning hydrogenations [49], cycloaddition reactions [50], hydrosilylations [51], hydroxylation and hydrogenolysis [52], oxidation of CO and CO/H₂ [53], oxidative acetoxylation [54], McMurry [55], Suzuki [56], Heck-Type [57] couplings and enantioselective hydrogenations [58]. Two main reasons for the nanoclusters used as catalyst are caused by a large percentage of a nanocluster’s metal atoms lie on the surface, and that surface atoms do not necessarily order themselves in the same way

that those in the bulk do. So nanoclusters give the opportunity to control both the nanocluster size and the surface ligands [45].

Transition-metal nanoclusters tender to go in bulk metal in aqueous medium which brings a necessity of the stabilization process with suitable stabilizers thinking of the long-term solution and solid-state (e.g., storage) stability, if practical applications of metal nanoclusters are to be realized [59].

3.2. Stabilization of Metal Nanoparticles

3.2.1. Electrostatic Stabilization

In 1940, Derjaguin, Landau, Verwey, and Overbeek developed a theory to explain stabilization of colloids. They named the theory as DLVO [60] which is explained by adsorption of anions by the coordinatively unsaturated, electrophilic surface of nanocolloids to succeed Coulombic repulsion between particles. Therefore, van der Waals forces which lead to aggregation of particles are resisted by this electrostatic repulsion. Thus, DLVO stabilization type is commonly referred to as electrostatic stabilization [47].

Electrostatic stabilization can be achieved by dissolving (mostly aqueous) ionic compounds like halides, carboxylates, or polyoxoanions in solution [61]. The main reason for the formation of electrostatic stabilization is the formation of electrical double layer that is formed by the anions and cations interacting with the metallic particle surface which results in a coulombic repulsion between particles. Electrostatic repulsion will help particles not to aggregate, if electric potential formed by the double layer is high enough. Whereas, changing total charge on the metal cluster surface can modify the degree of stabilization, and solvent polarity has an influence on the degree of particle dispersion [65] Fig. 3.1. shows the schematic representation of electrostatic stabilization.

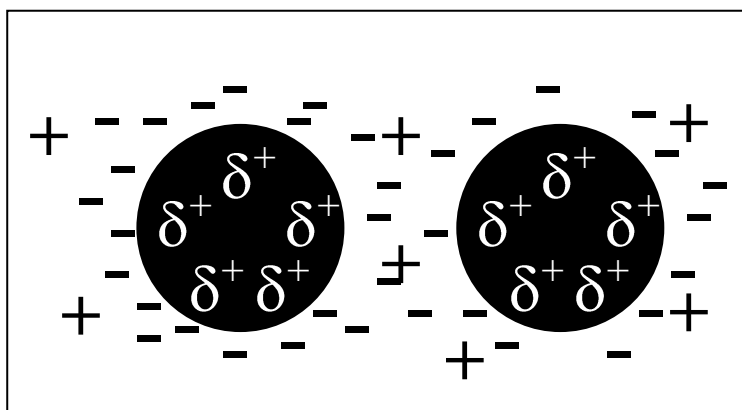


Figure 3.1. Schematic representation of electrostatic stabilization

3.2.2. Steric Stabilization

Steric stabilization can be achieved by adsorption of large organic molecules on the surface of the nanoparticle. These large organic molecules are polymers like poly(N-vinyl-2-pyrrolidone) (PVP), dendrimers and large alkylammonium cations [62]. These large adsorbates provide a steric barrier which prevents close contact of the metal particle centers [65]. Fig.3.2.

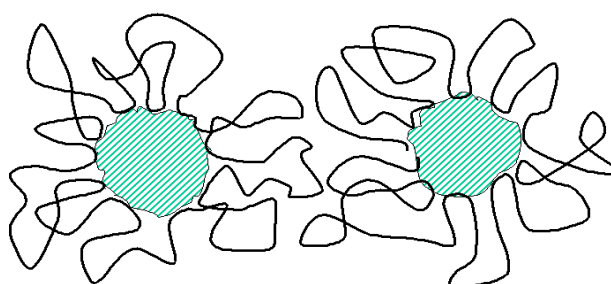


Figure 3.2. Schematic representation of steric stabilization

Polymeric stabilizers occupy many weak bonds with the nanoparticle's surface rather than forming less strong bonds at specific sites of the particles. This type of stabilization is very versatile[63].

3.3. Preparation of Metal Nanoparticles

“Mechanic subdivision of metallic aggregates (physical-as noted top down method)” and “nucleation and growth of metallic atoms (chemical-as noted bottom up method)” are the methods that can be used to prepare dispersed metallic nanoparticles. These two methods include lots of sub-methods for the preparation of metal nanoparticles. However, chemical methods are more efficient since physical methods have some constraints on the forming broad-range particle size (>10 nm generally) and also, they can not be prepared to give reproducible catalysts⁶⁴. Moreover, chemical methods give opportunity to control over size like reduction of transition metal salts. This is very important because nanoclusters should be or have at least (i) specific size (1-10nm), (ii) well-defined surface composition, (iii) reproducible synthesis and properties, and (iv) isolable and redispersible [45]. Chemical reduction of transition metal salts, thermolysis, photolysis, radiolysis, displacement of ligands from organometallic complexes and reduction by electrochemical methods are the some nanocluster synthesis methods [23].

3.3.1. Chemical Reduction of Transition Metal Salts

For the formation of colloidal suspensions of metals, reduction of transition metal salts in solution is the most extensively used method which is very simple to generate. Extended range of reducing agents can be used for the reduction like hydrogen or carbon monoxide as gas, sodium borohydride or sodium citrate as hydrides or salts, or alcohols as oxidable solvents [61].

3.3.2. Reduction by Electrochemical Methods

Reduction by electrochemical methods contains a large-scale synthetic procedure which enables to synthesize size-controlled particles and their isolation from solution is very easy and this synthesis give good yields (>95%)⁶¹.

3.3.3. Displacements of Ligands from Organometallic Complexes

Colloidal suspension of metals can be formed by changing some zerovalent organometallic complexes with the help of reduction or ligands displacements [61].

3.4. Characterization of Metal Nanoparticles

Characterization of metal nanoparticles is another important subject for the nanoparticle chemistry since characterization of nanoclusters is directly related to the particle size and overall composition. Generally used characterization techniques are; transmission electron microscopy (TEM), UV-Visible spectroscopy (UV-Vis), nuclear magnetic resonance spectroscopy (NMR), infrared spectroscopy (IR), elemental analysis, and energy dispersive spectroscopy (EDS). On the other hand, analytical ultracentrifugation-sedimentation, extended X-ray absorption fine structure (EXAFS), scanning tunnelling microscopy (STM), atomic force microscopy (AFM), high performance liquid chromatography (HPLC), light scattering, time-of-flight mass spectrometry, magnetic susceptibility, electrophoresis and ion-exchange chromatography are the another characterization techniques that are used less than TEM, UV-Vis, NMR, IR and EDS [45]. As a more widely used characterization technique, TEM give chance to identify information about size, structure, morphology and state of aggregation of metal particles. But only TEM results are not enough to conclude about the catalyst nature [65]. Figure 3.3. shows the complete picture of methods used for the characterization of nanoparticles.

In this study, TEM, UV-Vis, FT-IR and XPS were used for the characterization of Co(0) nanoclusters.

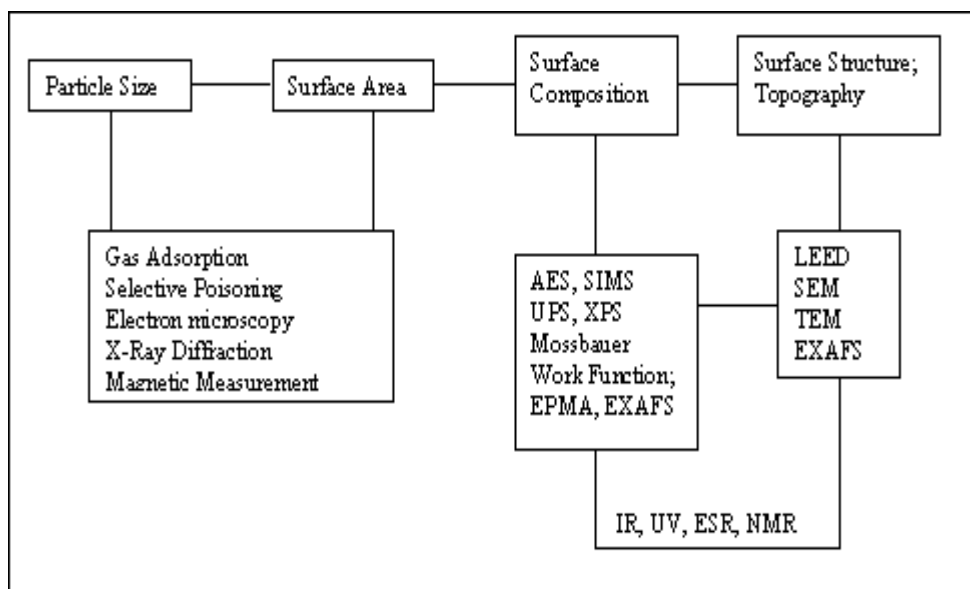


Figure 3.3 : Common methods available for nanoparticles characterization

CHAPTER 4

EXPERIMENTAL

4.1. Materials

Cobalt(II) chloride hexahydrate ($\text{CoCl}_2 \cdot 6\text{H}_2\text{O}$) (98%), sodium borohydride (98%) were purchased from Aldrich[®], polyacrylic acid ($\text{C}_3\text{H}_4\text{O}_2$) was purchased from Fluka and sodium phosphate ($\text{Na}_3\text{PO}_4 \cdot 12\text{H}_2\text{O}$) was purchased from Riedel-De Haen AG Hannover. Deionized water was distilled by water purification system (Şimşek SL-200, Ankara, Turkey). All glassware and Teflon coated magnetic stir bars were cleaned with acetone, followed by copious rinsing with distilled water before drying in an oven at 150 °C.

4.2 In-situ Formation of Hydrogenphosphate-stabilized Cobalt(0) Nanoclusters and Catalytic Hydrolysis of Sodium Borohydride

In-situ formation of hydrogenphosphate-stabilized cobalt(0) nanoclusters and catalytic hydrolysis of sodium borohydride were performed in the same medium. Before starting the experiment, a jacketed reaction flask (75 mL) containing a Teflon-coated stir bar was placed on a magnetic stirrer (Heidolph MR-301) and thermostated to 25.0 ± 0.1 °C by circulating water through its jacket from a constant temperature bath (Lauda RL6). Then, a graduated glass tube (50 cm in height and 4.7 cm in diameter) filled with water was connected to the reaction flask to measure the volume of the hydrogen gas to be evolved from the reaction. Next, 284 mg (7.47 mmol) NaBH_4 (corresponding to 30 mmol = 672 mL H_2 at 25.0 ± 0.1 °C and 0.91 atm pressure) and 79.8 mg (0.21 mmol) $\text{Na}_3\text{PO}_4 \cdot 12\text{H}_2\text{O}$ were dissolved in 40 mL water. The solution was transferred with

a 50 mL glass-pipette into the reaction flask thermostated at 25.0 ± 0.1 °C. Then, 10 mL aliquot of 7.0 mM cobalt(II) chloride solution was transferred into the reaction flask using a 10 mL gastight syringe and the solution was stirred at 1200 rpm. The initial concentrations of NaBH₄ and cobalt(II) chloride were 150 mM (7.5 mmol) and 1.4 mM (0.07 mmol), respectively. Molar ratio of NaBH₄ to CoCl₂·6H₂O greater than 100 was used to ensure complete reduction of Co⁺² to its zero oxidation state and to observe the catalytic hydrolysis of sodium borohydride at the same time. A fast color change from pale purple to dark brown was observed indicating the formation of cobalt(0) nanoclusters. When the nanoclusters formation was completed (within less than 1 minute) the catalytic hydrolysis was started to be measured by monitoring the volume of hydrogen gas evolved. The volume of hydrogen gas evolved was measured by recording the displacement of water level every 5 minutes at constant pressure. The reaction was ceased when 75% conversion was achieved. No bulk metal formation was observed during the catalytic hydrolysis reaction.

4.3. In-situ Formation of Poly(acrylic acid)-stabilized Cobalt(0) Nanoclusters and Catalytic Hydrolysis of Sodium Borohydride

In-situ formation of poly(acrylic acid)-stabilized cobalt(0) nanoclusters and catalytic hydrolysis of sodium borohydride were performed in the same medium. Before starting the experiment, a jacketed reaction flask (75 mL) containing a Teflon-coated stir bar was placed on a magnetic stirrer (Heidolph MR-301) and thermostated to 25.0 ± 0.1 °C by circulating water through its jacket from a constant temperature bath (Lauda RL6). Then, a graduated glass tube (50 cm in height and 4.7 cm in diameter) filled with water was connected to the reaction flask to measure the volume of the hydrogen gas to be evolved from the reaction. Next, 284 mg (7.47 mmol) NaBH₄ (corresponding to 30 mmol = 672 mL H₂ at 25.0 ± 0.1 °C and 0.91 atm pressure) and 15,12 mg (0.07 mmol) [C₃H₄O₂]_n were dissolved in 40 mL water. The solution was transferred with a 50 mL glass-pipette into the reaction flask thermostated at 25.0 ± 0.1 °C. Then, 10 mL aliquot of 7.0 mM cobalt(II) chloride solution was transferred into the reaction flask using a 10 mL gastight syringe and

the solution was stirred at 1200 rpm. The initial concentrations of NaBH₄ and cobalt(II) chloride were 150 mM (7.5 mmol) and 1.4 mM (0.07 mmol), respectively. Molar ratio of NaBH₄ to CoCl₂·6H₂O greater than 100 was used to ensure complete reduction of Co⁺² to its zero oxidation state and to observe the catalytic hydrolysis of sodium borohydride at the same time. A fast color change from pale purple to dark brown was observed indicating the formation of cobalt(0) nanoclusters. When the nanoclusters formation was completed (within less than 1 minute) the catalytic hydrolysis was started to be measured by monitoring the volume of hydrogen gas evolved. The volume of hydrogen gas evolved was measured by recording the displacement of water level every 1 minute at constant pressure. The reaction was ceased when 75% conversion was achieved. No bulk metal formation was observed during the catalytic hydrolysis reaction.

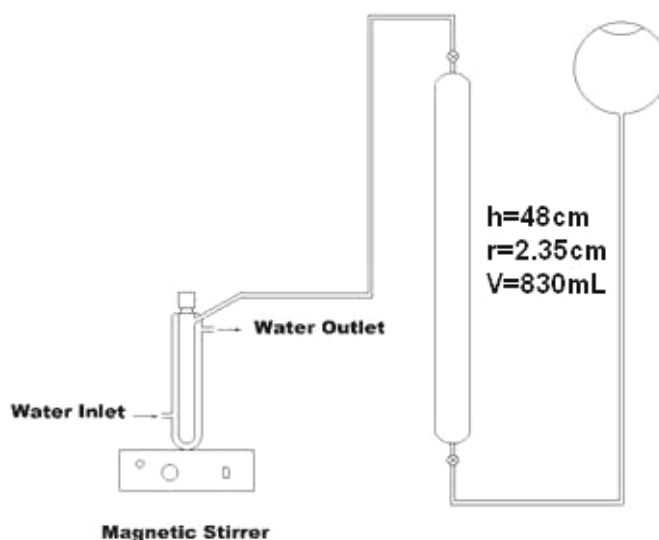


Figure 4.1. The experimental setup used in performing the catalytic hydrolysis of sodium borohydride and measuring the hydrogen generation rate.

4.4. Self-Hydrolysis Of Sodium Borohydride

In a 100 mL beaker, 284 mg sodium borohydride was dissolved in 2 mL water and the volume of the solution was adjusted to 50 mL by adding water. The solution was then transferred with a pipette into the reaction flask thermostated at 25.0 ± 0.1 °C. The experiment was started by closing the reaction flask and turning on the stirring at 1200 rpm simultaneously, exactly in the same way as described in the previous section. The volume of hydrogen gas generated was measured every 5 minutes.

4.5. Kinetics Of Hydrogenphosphate-Stabilized Cobalt(0) Nanocluster In Catalytic Hydrolysis Of Sodium Borohydride

In order to establish the rate law for catalytic hydrolysis of NaBH_4 using hydrogenphosphate-stabilized cobalt(0) nanoclusters, two different sets of experiments were performed in the same way as described in the section “In-situ formation of hydrogenphosphate-stabilized cobalt(0) nanoclusters and catalytic hydrolysis of sodium borohydride”. In the first set of experiments, the hydrolysis reaction was performed starting with different initial concentration of cobalt(II) chloride (1.0, 1.2, 1.4, 1.6, 1.8, 2.0 mM) and keeping the initial sodium borohydride concentration constant at 150 mM. The second set of experiments were performed by keeping the initial concentration of cobalt(II) chloride constant at 1.4 mM and varying the NaBH_4 concentration between 150, 300, 450, 600 and 750 mM to provide a substrate to catalyst ratio of 100 at least. Finally, the catalytic hydrolysis of NaBH_4 was performed in the presence of Co(0) nanoclusters at constant substrate (150 mM) and catalyst (1.4 mM) concentrations at various temperatures in the range of 20-40 °C in order to obtain the activation energy (E_a), enthalpy (ΔH^\ddagger), and entropy (ΔS^\ddagger).

4.6. Kinetics Of Poly(acrylic acid)-Stabilized Cobalt(0) Nanocluster In Catalytic Hydrolysis Of Sodium Borohydride

In order to establish the rate law for catalytic hydrolysis of NaBH₄ using poly(acrylic acid)-stabilized cobalt(0) nanoclusters, two different sets of experiments were performed in the same way as described in the section “In-situ formation of poly(acrylic acid)-stabilized cobalt(0) nanoclusters and catalytic hydrolysis of sodium borohydride”. In the first set of experiments, the hydrolysis reaction was performed starting with different initial concentration of cobalt(II) chloride (1.0, 1.5, 2.0, 2.5, 3.0, 3.5 mM) and keeping the initial sodium borohydride concentration constant at 150 mM. The second set of experiments were performed by keeping the initial concentration of cobalt(II) chloride constant at 1.4 mM and varying the NaBH₄ concentration between 150, 300, 450, 600 and 750 to provide a substrate to catalyst ratio of 100 at least. Finally, the catalytic hydrolysis of NaBH₄ was performed in the presence of Co(0) nanoclusters at constant substrate (150 mM) and catalyst (1.4 mM) concentrations at various temperatures in the range of 20-40 °C in order to obtain the activation energy (E_a), enthalpy (ΔH^\ddagger), and entropy (ΔS^\ddagger).

4.7. Effect Of Hydrogenphosphate Concentration On The Catalytic Activity Of Cobalt(0) Nanoclusters

In order to study the effect of hydrogenphosphate concentration on the catalytic activity of cobalt(0) nanoclusters in the hydrolysis of sodium borohydride (150 mM), catalytic activity tests were performed at 25.0 ± 0.1 °C starting with various concentrations of sodium phosphate (1.4, 2.8, 4.2, 5.6 and 7.0 mM) in the in-situ generation of cobalt(0) nanoclusters. In all the experiments the total volume of solution was kept constant at 50 mL. All the experiments were performed in the same way as described in the section “In-situ formation of hydrogenphosphate-stabilized cobalt(0) nanoclusters and catalytic hydrolysis of sodium borohydride”.

4.8. Effect Of Poly(acrylic acid) Concentration On The Catalytic Activity Of Cobalt(0) Nanoclusters

In order to study the effect of poly(acrylic acid) concentration on the catalytic activity of cobalt(0) nanoclusters in the hydrolysis of sodium borohydride (150 mM), catalytic activity tests were performed at 25.0 ± 0.1 °C starting with various concentrations of poly(acrylic acid) (1.4, 2.8, 4.2, 5.6 and 7.0 mM) in the in-situ generation of cobalt(0) nanoclusters. In all the experiments the total volume of solution was kept constant at 50 mL. All the experiments were performed in the same way as described in the section “In-situ formation of poly(acrylic acid)-stabilized cobalt(0) nanoclusters and catalytic hydrolysis of sodium borohydride”.

4.9. Catalytic Lifetime Of Hydrogenphosphate-Stabilized and Poly(acrylic acid)-Stabilized Cobalt(0) Nanoclusters

The catalytic lifetime of hydrogenphosphate stabilized and poly(acrylic acid) stabilized cobalt(0) nanoclusters in the hydrolysis of sodium borohydride were determined by measuring the total turnover number (TTO). Such a lifetime experiment was started with a 50 mL solution containing 1.0 mM cobalt(II) chloride and 150 mM NaBH₄ at 25.0 ± 0.1 °C. The nanocluster formation and hydrolysis of sodium borohydride reaction was continued until hydrogen gas evolution was slowed down to the self hydrolysis level. Hydrogenphosphate stabilized cobalt(0) nanoclusters could provide 1285 total turnovers over 4 hours and poly(acrylic acid) stabilized cobalt(0) nanoclusters could provide 6600 turnovers for the hydrolysis of sodium borohydride over 36 hours before deactivation.

4.10. Characterization of Hydrogenphosphate-Stabilized and Poly(acrylic acid)-Stabilized Cobalt(0) Nanoclusters

4.10.1. TEM Analysis

TEM Sample Preparation; The samples used for the TEM experiments were harvested from the preparation of hydrogen phosphate-stabilized cobalt(0) nanoclusters solution and poly(acrylic acid) stabilized cobalt(0) nanoclusters as described above: a 5-mL aliquots of hydrogen phosphate and poly(acrylic acid) stabilized cobalt(0) nanoclusters' solutions in water were transferred into a clean screw-capped glass vial with a disposable polyethylene pipette, separately. The colloidal solutions were deposited on the silicon oxide coated copper TEM grids by immersing the grids into the solutions for 5 s and then evaporating the volatiles from the grids under inert gas atmosphere. This samples on the grid were then sealed under N₂.

TEM Analysis; Transmission electron microscopy images were taken at Brown University Chemistry Laboratory by using Hitachi H7600T TEM instrument operating at 120 kV and with a 2.0Å point-to-point resolution. Samples were examined at magnification between 100 and 500k.

4.10.2. XPS (X-Ray photoelectron spectroscopy)

XPS Sample Preparation; After catalysis, described in the previous section, 10 mL aliquots of hydrogenphosphate-stabilized cobalt(0) nanoclusters solution were transferred via disposable pipette into eight new 15×100 mm glass tubes separately and all the samples were simultaneously centrifuged (Heraeus Labofuge 200) for 2 hours. After the decantation of the supernatant solution, the precipitates were dried under vacuum for 2 hours. The dry samples of cobalt(0) nanoclusters were collected in a screw-capped glass vial and sent to the METU Central Laboratory for XPS

analysis. Same preparation steps were also followed for the poly(acrylic acid) stabilized cobalt(0) nanoclusters' XPS sample preparation.

XPS Analysis; X-ray photoelectron spectrum (XPS) was taken at the Middle East Technical University Central Laboratory using SPECS spectrometer equipped with a hemispherical analyzer and using monochromatic Mg-K α radiation (1250.0 eV, the X-ray tube working at 15 kV and 350 W) and pass energy of 48 eV.

4.10.3. FT-IR Spectra

The samples prepared for the XPS analysis were also used for taking the FTIR spectra. FTIR spectra of the hydrogenphosphate-stabilized and poly(acrylic acid) stabilized cobalt(0) nanoclusters were taken from KBr pellet on a Bruker FRA 20 FTIR Spectrophotometer using Opus software.

4.10.4. UV-vis Study

In two glass vials, 10 mL aqueous solution of 0.14 mM CoCl₂.6H₂O (purple in color) and 10 mL of aqueous solution 0.42 mM Na₃PO₄ and 0.14 mM CoCl₂.6H₂O mixture were prepared. In another glass vial, 10 mL aqueous solution of 0.42 mM Na₃PO₄, 0.14 mM CoCl₂.6H₂O and 150 mM NaBH₄ was prepared and waited for the nanocluster formation. UV-visible spectrum of the CoCl₂.6H₂O (precursor), mixture of Na₃PO₄.12H₂O and CoCl₂.6H₂O and nanocluster was taken with a Hewlett Packard 8452A Model Diode Array Spectrophotometer with kinetics program of UV-Visible ChemStation software. Data was collected and graphed with using Microsoft Excel 2003 for the UV-vis study of hydrogen phosphate stabilized Co(0) nanoclusters catalysts. On the other hand, in another two glass vials, 10 mL aqueous solution of 0.14 mM CoCl₂.6H₂O (purple in color) and 10 mL of aqueous solution 0.42 mM poly(acrylic acid) and 0.14 mM CoCl₂.6H₂O mixture were prepared. In another glass vial, 10 mL aqueous solution of 0.42 mM poly(acrylic acid), 0.14 mM CoCl₂.6H₂O and 150 mM NaBH₄ was prepared and waited for the nanocluster formation. UV-visible spectrum of the CoCl₂.6H₂O (precursor), mixture of

$\text{Na}_3\text{PO}_4 \cdot 12\text{H}_2\text{O}$ and $\text{CoCl}_2 \cdot 6\text{H}_2\text{O}$ and nanocluster was taken with a Hewlett Packard 8452A Model Diode Array Spectrophotometer with kinetics program of UV-Visible ChemStation software. Data was collected and graphed with using Microsoft Excel 2003 for the poly(acrylic acid) stabilized Co(0) nanoclusters catalysts.

CHAPTER 5

RESULTS AND DISCUSSION

5.1. In-Situ Formation of Hydrogen Phosphate-stabilized and Poly(acrylic acid)-stabilized Cobalt(0) Nanoclusters and Catalytic Hydrolysis of Sodium Borohydride

The hydrogen phosphate stabilized and poly(acrylic acid)-stabilized cobalt(0) nanoclusters were formed in situ during the hydrolysis of sodium borohydride. The color change and the UV–vis electronic absorption spectra show that the reduction of precursor complex is fast and without an observable induction period the hydrolysis of sodium borohydride starts immediately releasing hydrogen gas. Figure 5.1 shows the UV–visible electronic absorption spectra of solutions containing cobalt(II) ion in the presence of hydrogen phosphate stabilizer in aqueous solution before and after reduction by sodium borohydride. The UV–visible spectrum of cobalt(II) chloride exhibits an absorption band at 510 nm, attributable to d–d transition. After reduction, this d-d transition band of cobalt(II) ion disappears.

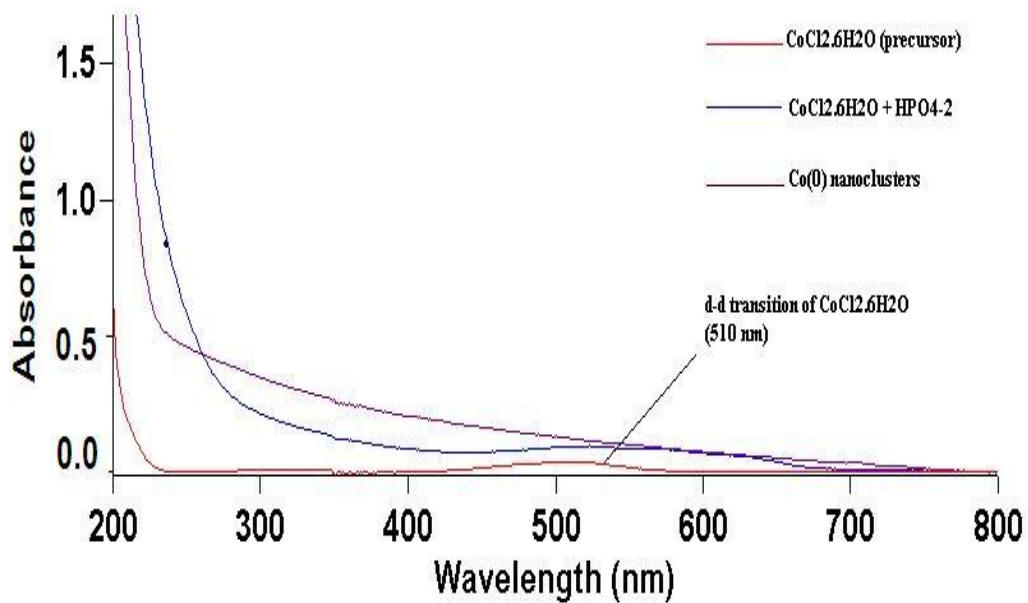


Figure 5.1. UV-visible spectra of hydrogen phosphate stabilized Co(0) nanoclusters

In the case of poly(acrylic acid)-stabilized cobalt(0) nanoclusters, after reduction by sodium borohydride, this transition band of cobalt(II) ion disappears (Figure 5.2).

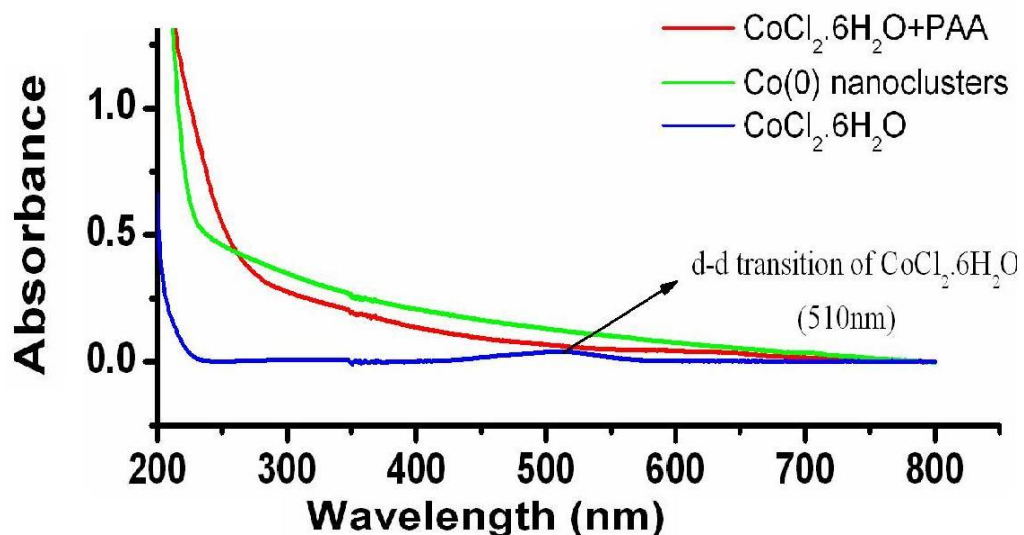


Figure 5.2. UV-visible spectra of poly(acrylic acid) stabilized Co(0) nanoclusters

Cobalt(0) nanoclusters formed from the reduction of the respective precursor complex by sodium borohydride in the presence of electrostatic and steric stabilizers are stable in aqueous solution. No bulk metal formation was observed in solution standing for weeks at room temperature in inert gas atmosphere. The hydrogen phosphate stabilized and poly(acrylic acid)-stabilized cobalt(0) nanoclusters can be isolated from the reaction solution as dark brown solid by removing the volatiles in vacuum.

The morphology and particle size of hydrogen phosphate stabilized and poly(acrylic acid) stabilized Co(0) nanoclusters were studied by using TEM images. Figure 5.3 and Figure 5.4 show the TEM images and corresponding histograms of cobalt(0) nanoclusters prepared from the reduction of cobalt(II) chloride hexahydrate (1.4 mM) by sodium borohydride in the presence of hydrogen phosphate (4.2mM) and poly(acrylic acid) (4.2 mM).

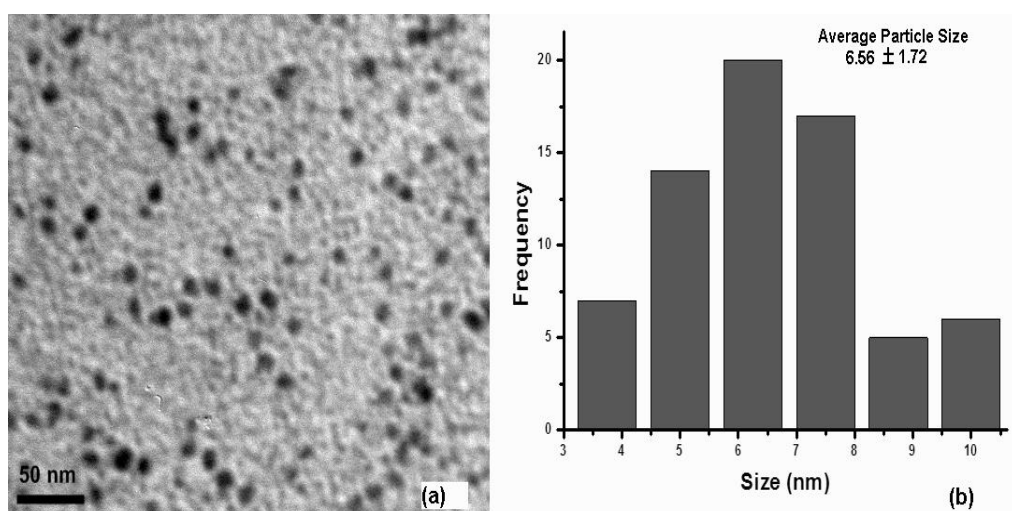


Figure 5.3. (a) TEM image and (b) associated histogram of hydrogen phosphate stabilized cobalt(0) nanoclusters

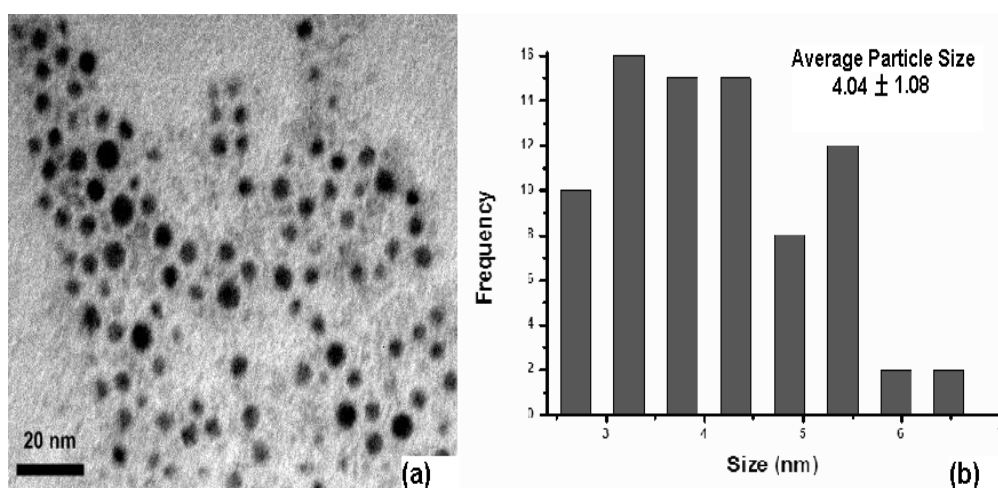


Figure 5.4. (a) TEM image and (b) associated histogram of poly(acrylic acid) stabilized cobalt(0) nanoclusters

In the TEM images 69 and 80 non-touching particles were counted for the construction of histograms, separately. The particle size of hydrogen phosphate stabilized cobalt(0) nanoclusters ranges from 3.5 nm to 10.0 nm with a mean value of

6.6 nm. On the other hand, poly(acrylic acid) stabilized cobalt(0) nanoclusters' particle size ranges from 1.1 nm to 6.5 nm where mean value equals to 4.0 nm.

5.2. Effect of Hydrogen Phosphate and Poly(acrylic acid) Concentration on the Stability and Activity of Cobalt(0) Nanoclusters Catalyst

Effect of the stabilizer concentration on the stability and catalytic activity of the cobalt(0) nanoclusters catalyst was investigated by performing the catalytic hydrolysis of sodium borohydride starting with 1.4 mM cobalt(II) ion and different hydrogenphosphate ion concentration. Figure 5.5 shows the volume of hydrogen generated versus time plot for the hydrolysis of sodium borohydride catalyzed by hydrogenphosphate-stabilized cobalt(0) nanoclusters starting with various concentration of hydrogenphosphate ion at 25.0 ± 0.1 °C.

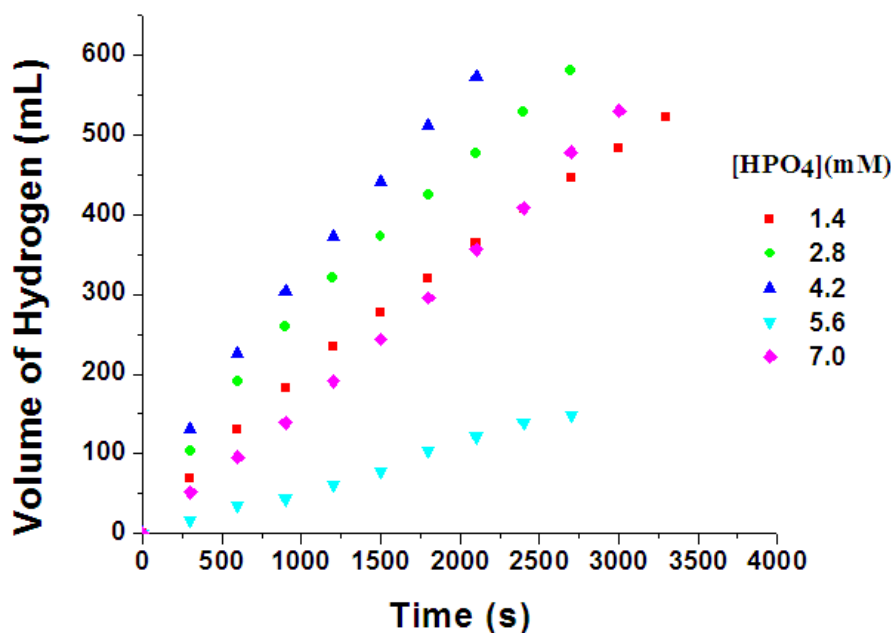


Figure 5.5. The graph of volume of hydrogen versus time for the hydrolysis of sodium borohydride catalyzed by hydrogen phosphate-stabilized cobalt(0) nanoclusters starting with various hydrogenphosphate concentrations at 25 ± 0.1 °C.

[Co] = 1.4 mM, [NaBH₄] = 150 mM .

Generation of hydrogen starts immediately and continues almost linearly. Figure 5.6 shows that the hydrogen generation rate, measured from the nearly linear portion of the curves in Figure 5.5, increases with the increasing concentration of hydrogen phosphate until 4.2 mM of hydrogen phosphate concentration ($[\text{HPO}_4]/[\text{Co}] = 3$). However, at the concentrations higher than 4.2 mM, the reaction rate decreases. This indicates that the highest catalytic activity of hydrogen phosphate-stabilized cobalt(0) nanoclusters was obtained at the ratio of hydrogen phosphate to cobalt equals 3. Thus, the hydrogen phosphate concentration of 4.2 mM, corresponding to a hydrogen phosphate to cobalt ratio of 3, was selected for the further experiments.

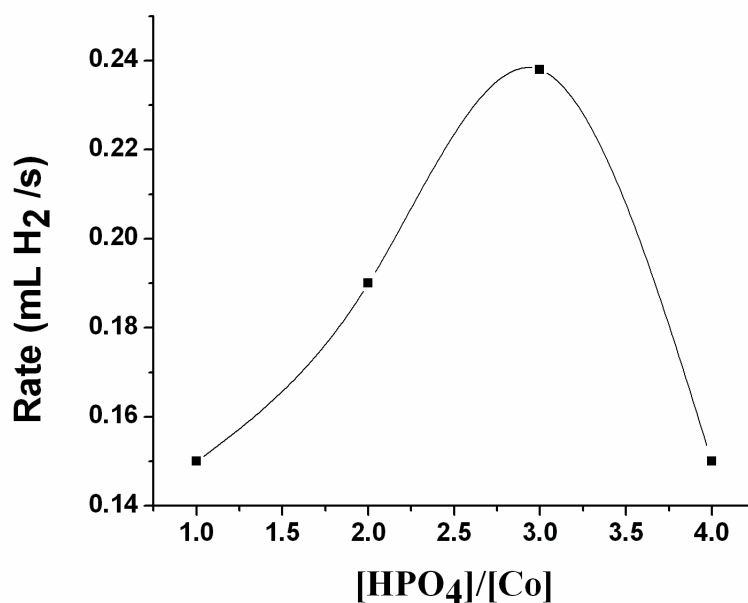


Figure 5. 6. Hydrogen generation rate versus $[\text{HPO}_4]/[\text{Co}]$ ratio at 25.0 ± 0.1 °C

Effect of the stabilizer concentration on the stability and catalytic activity of the cobalt(0) nanoclusters catalyst was also investigated by performing the catalytic hydrolysis of sodium borohydride starting with 1.4 mM cobalt(II) ion and different poly(acrylic acid) concentrations. Figure 5.7 shows the volume of hydrogen generated versus time plot for the hydrolysis of sodium borohydride catalyzed by

cobalt(0) nanoclusters starting with various concentration of poly(acrylic acid) at 25.0 ± 0.1 °C.

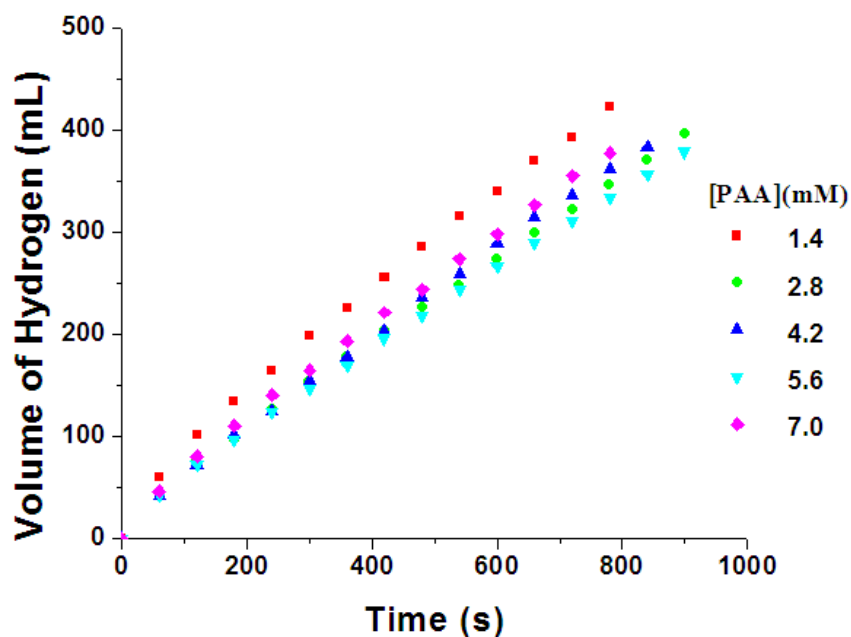


Figure 5.7. The graph of volume of hydrogen versus time for the hydrolysis of sodium borohydride catalyzed by cobalt(0) nanoclusters starting with various poly(acrylic acid) concentrations at 25 ± 0.1 °C. $[\text{Co}] = 1.4$ mM, $[\text{NaBH}_4] = 150$ mM

A rapid hydrogen generation starts immediately at all of the poly(acrylic acid) concentrations. The hydrogen generation continues almost linearly and then slows down as the substrate concentration decreases toward the end of reaction. Figure 5.8 shows that the hydrogen generation rate, measured from the nearly linear portion of the curves in Figure 5.7., decreasing with the increasing concentration of poly(acrylic acid). This indicates that the catalytic activity of cobalt(0) nanoclusters decreases with the increasing concentration of stabilizer as expected [66].

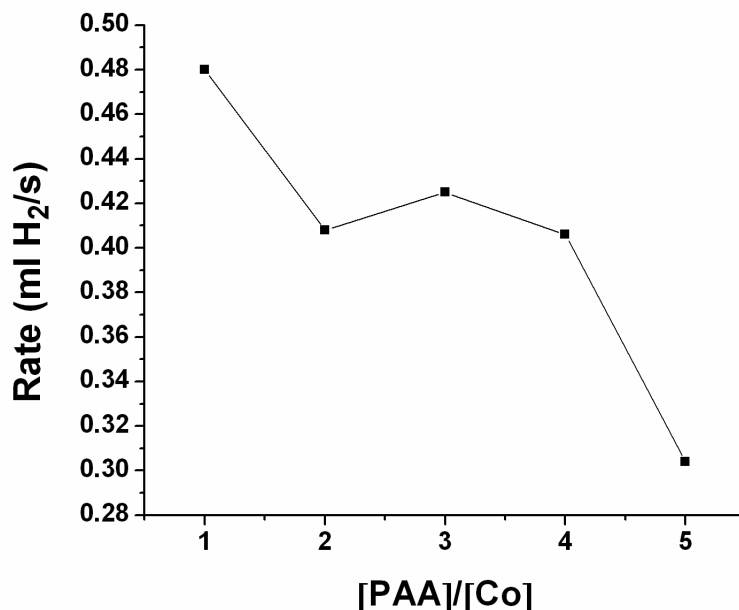


Figure 5. 8. Hydrogen generation rate versus [PAA]/[Co] ratio at 25.0 ± 0.1 °C

Highest catalytic activity is observed at the 1:1 ratio of [poly(acrylic acid)]/[cobalt] where the concentration is equal to 1.4 mM. However, during different temperature experiments it is observed that 1:1 ratio of [poly(acrylic acid)]/[cobalt] nanoclusters decomposes where they show the aggregation behaviour. For this reason, 1:3 ratio of [cobalt]/ [poly(acrylic acid)] is used for the further sets of experiments in which high catalytic activity and stability are observed both at the poly(acrylic acid) concentration of 4.2 mM.

5.3. Reduction of Cobalt(II) Chloride by Sodium Borohydride

The formation of cobalt in zero oxidation state from reduction of cobalt(II) chloride by sodium borohydride was shown by XPS. Figure 5.9 shows the XPS spectrum of hydrogenphosphate-stabilized cobalt(0) nanoclusters prepared in aqueous solution from the reduction of cobalt(II) chloride (1.4 mM) by sodium borohydride (150 mM) in the presence of hydrogenphosphate (4.2 mM) at 25 ± 0.1 °C. And also, Figure 5.10 shows the XPS spectrum of poly(acrylic acid)-stabilized

cobalt(0) nanoclusters prepared in aqueous solution from the reduction of cobalt(II) chloride (1.4 mM) by sodium borohydride (150 mM) in the presence of poly(acrylic acid) (4.2 mM) at 25 ± 0.1 °C.

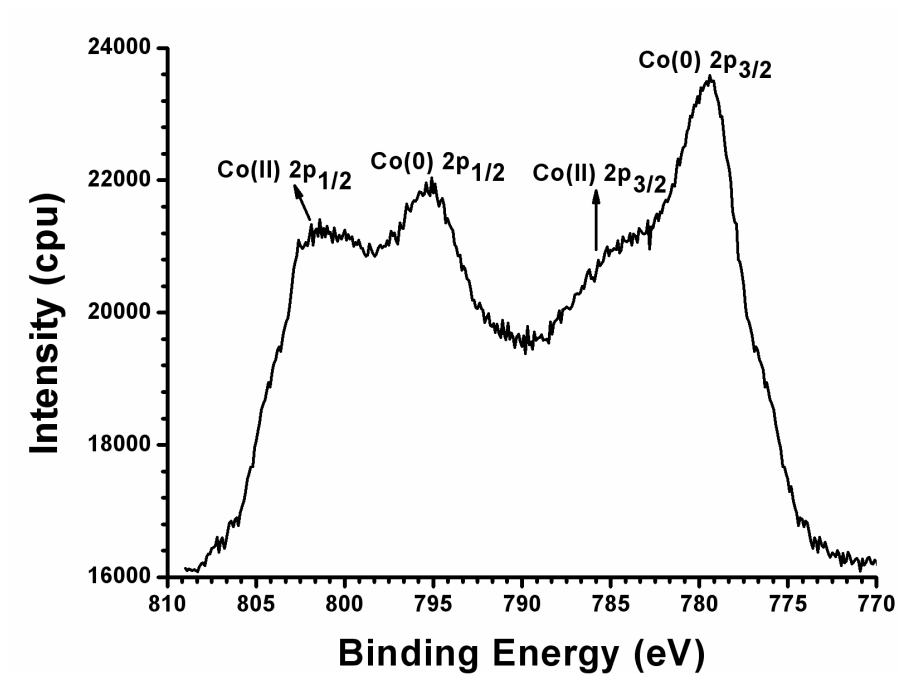


Figure 5.9. XPS spectrum of hydrogenphosphate-stabilized cobalt(0) nanoclusters

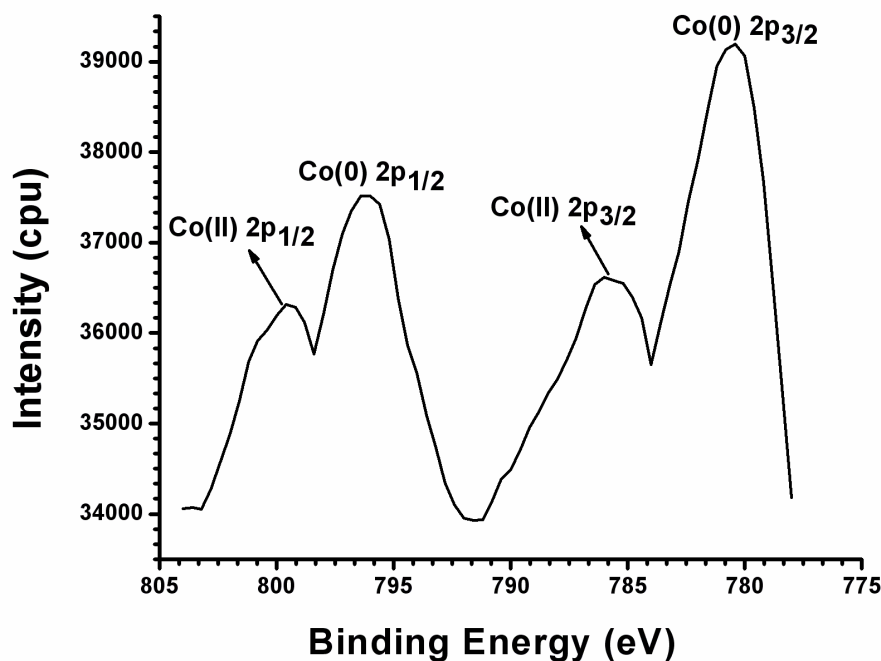


Figure 5.10. XPS spectrum of poly(acrylic acid)-stabilized cobalt(0) nanoclusters

The XPS spectrum in Figure 5.9 exhibits two bands at 779.3 eV and 795.3 eV and Figure 5.10 exhibits two bands at 780.8 and 796.3 which can be assigned to Co(0) 2p_{3/2} and Co(0) 2p_{1/2}, respectively. Compared to the values for the bulk cobalt (778.0 and 793.0 eV, respectively) [67], the 2p_{3/2} and 2p_{1/2} binding energies are shifted to the higher values which can be explained by the matrix effect [68]. Additional higher energy bands were also observed in both of the spectra which are 801.5 eV and 785.7 eV in Figure 5.9 and 799.6 eV and 786.2 eV in Figure 5.10, though with relatively weak intensities. These bands can be attributed to Co(II) 2p_{3/2} and Co(II) 2p_{1/2}, respectively [67]. Co(II) species might have been formed while preparing the XPS sample due to the air sensitivity of cobalt species.

5.4. Integrity of Stabilizers

Integrity of hydrogenphosphate and poly(acrylic acid) stabilizers were examined by FT-IR spectroscopy. FT-IR spectra of the isolated hydrogenphosphate-stabilized cobalt(0) nanoclusters and that of the hydrogenphosphate ion in

$\text{Na}_2\text{HPO}_4 \cdot 7\text{H}_2\text{O}$ are displayed together in Figure 5.11., and poly(acrylic acid)-stabilized cobalt(0) nanoclusters and that of the poly(acrylic acid) ($[\text{C}_3\text{H}_4\text{O}_2]_n$) are displayed separately in Figure 5.12.

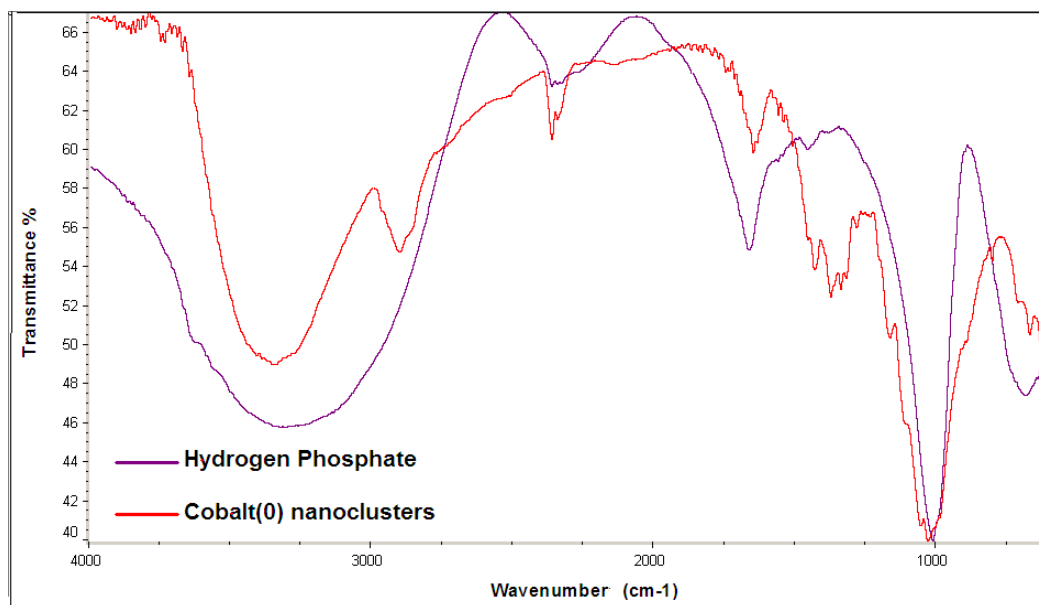


Figure 5.11. FT-IR Spectra of hydrogen phosphate-stabilized Co(0) nanoclusters

The hydrogenphosphate ion in $\text{Na}_2\text{HPO}_4 \cdot 7\text{H}_2\text{O}$ has characteristics bands at **$1000\text{-}1100\text{ cm}^{-1}$** . The comparison of IR spectra of free hydrogenphosphate and isolated hydrogenphosphate-stabilized cobalt(0) nanoclusters shows that hydrogenphosphate ions exist in the nanoclusters sample most probably on the surface of particles.

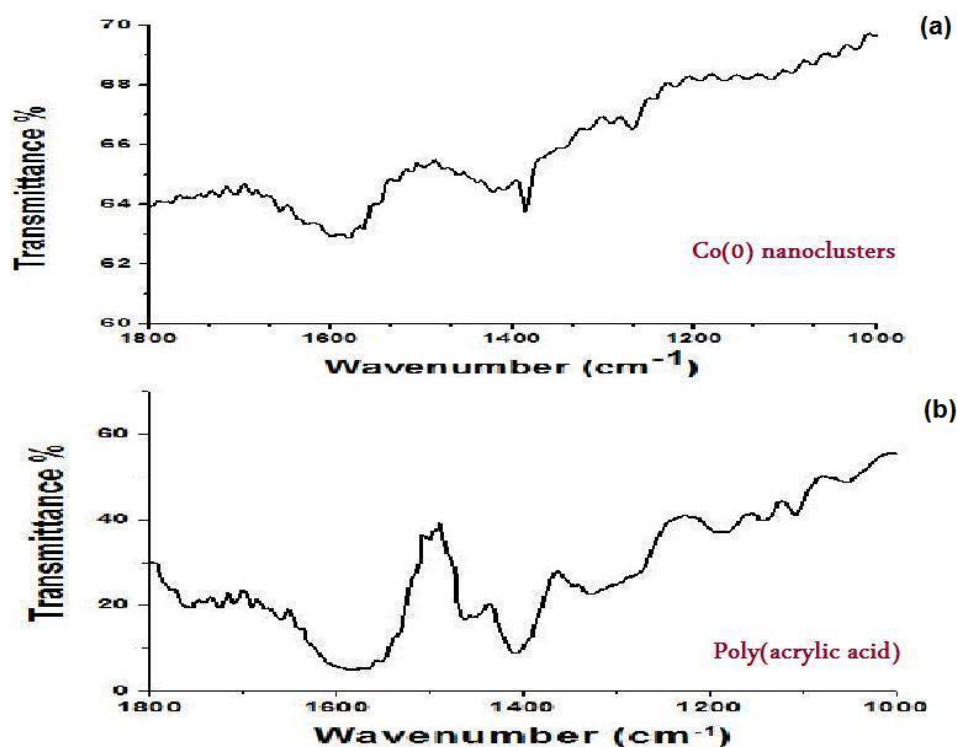


Figure 5.12. FT-IR Spectra of poly(acrylic acid)-stabilized Co(0) nanoclusters (a) Co(0) nanoclusters (b) Poly(acrylic acid)

The poly(acrylic acid) has characteristic band at **1690-1740 cm^{-1}** . The comparison of IR spectra of free poly(acrylic acid) and isolated poly(acrylic acid)-stabilized cobalt(0) nanoclusters shows that poly(acrylic acid) exist in the nanoclusters sample most probably on the surface of particles.

5.5. Lifetime of Catalyst

A catalyst lifetime experiment was performed starting with 1.0 mM cobalt(II) chloride nanoclusters and 150.0mM sodium borohydride in 50 mL aqueous solution at 25.0 ± 0.1 °C. It was found that the hydrogenphosphate-stabilized cobalt(0) nanoclusters provide 1285 turnovers of hydrogen gas generation from the hydrolysis of sodium borohydride over 4 hours before deactivation. This corresponds to a turnover frequency of 5.35 min^{-1} .

A catalyst lifetime experiment was also performed starting with 1.0 mM cobalt(II) chloride nanoclusters and 150.0 mM sodium borohydride in 50 mL aqueous solution at 25.0 ± 0.1 °C. It was found that the polyacrylic acid-stabilized cobalt(0) nanoclusters provide 6600 turnovers of hydrogen gas generation from the hydrolysis of sodium borohydride over 36 hours before deactivation. This corresponds to a turnover frequency of 3.05 min^{-1} .

5.6. Kinetics of Hydrolysis of Sodium Borohydride catalyzed by Hydrogen Phosphate-stabilized and Poly(acrylic acid)-stabilized Cobalt(0) Nanoclusters

It is well known that NaBH_4 hydrolyzes to give hydrogen gas spontaneously in water [69]. However, the hydrogen gas evolution rate is so slow compared to that of hydrolysis using cobalt(0) nanoclusters as catalyst. For example, in the absence of catalyst, the self hydrolysis of sodium borohydride liberates 94 mL of H_2 gas in 2 hours while sodium borohydride liberates 650.25 mL H_2 gas in the presence of 1.4 mM hydrogenphosphate-stabilized cobalt(0) nanoclusters in 55 minutes and 384.0mL H_2 gas in the presence of 1.4 mM poly(acrylic acid)-stabilized cobalt(0) nanoclusters in 14 minutes .

The hydrogenphosphate-stabilized and poly(acrylic acid)-stabilized cobalt(0) nanoclusters are found to be active catalyst for the hydrolysis of sodium borohydride at low concentrations and room temperature as shown in Figure 5.13. and Figure 5.14., which plots the volume of hydrogen generated versus time during the catalytic hydrolysis of 150 mM NaBH_4 solution in the presence of cobalt(0) nanoclusters in different concentrations at 25 ± 0.1 °C.

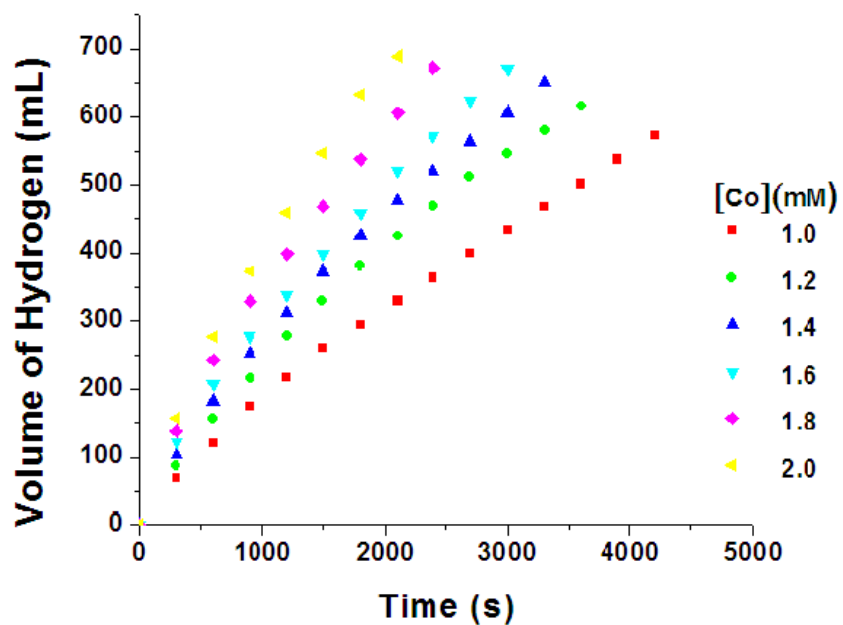


Figure 5.13. The graph of volume of hydrogen (mL) versus time (s) in different Co(II) chloride concentrations in all sets $[\text{NaBH}_4] = 150 \text{ mM}$ where in the presence of hydrogen phosphate as stabilizer

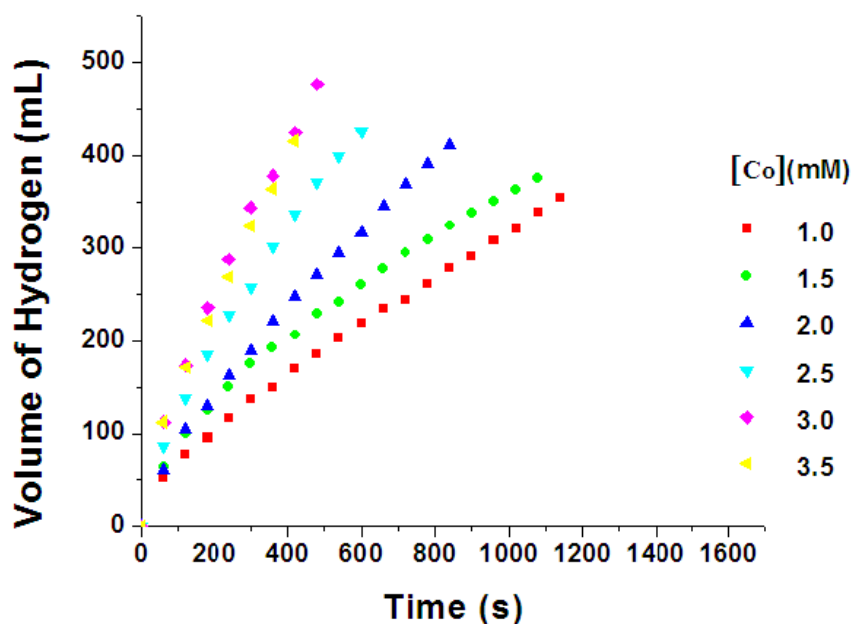


Figure 5.14. The graph of volume of hydrogen (mL) versus time (s) in different Co(II) chloride concentrations in all sets $[\text{NaBH}_4] = 150 \text{ mM}$ where in the presence of poly(acrylic acid) as stabilizer

The hydrogen generation rate was determined from the nearly linear portion of the plot for each cobalt(0) nanoclusters concentration experiment. Figure 5.15. shows the plot of hydrogen generation rate versus cobalt(II) chloride concentration, both in logarithmic scale. The slope of which is found to be $1.1315 \approx 1.0$ indicating that the hydrolysis reaction is first order with respect to the concentration of cobalt(0) nanoclusters catalyst where hydrogen phosphate used as stabilizer. In the second part of the experiment, where poly(acrylic acid) used as stabilizer, the hydrogen generation rate was determined from the nearly linear portion of the plot for each cobalt(0) nanoclusters concentration experiment, also. Figure 5.16. shows the plot of hydrogen generation rate versus cobalt(II) chloride concentration, both in logarithmic scale. The slope of which is found to be $1.0988 \approx 1.0$ indicating that the hydrolysis reaction is first order with respect to the concentration of cobalt(0) nanoclusters catalyst where poly(acrylic acid) used as stabilizer.

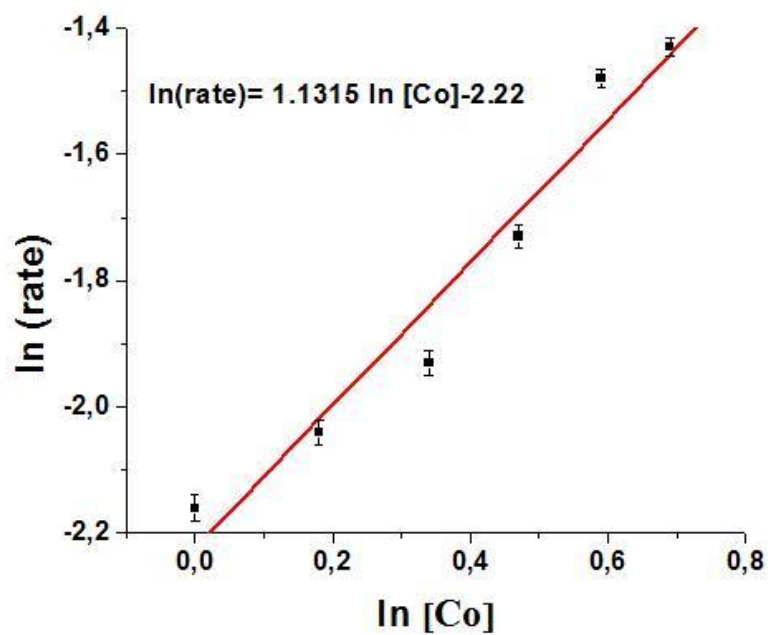


Figure 5.15. The graph of \ln Rate versus \ln [Co] at 25 °C and 150 mM NaBH_4 in the presence of hydrogenphosphate-stabilizer

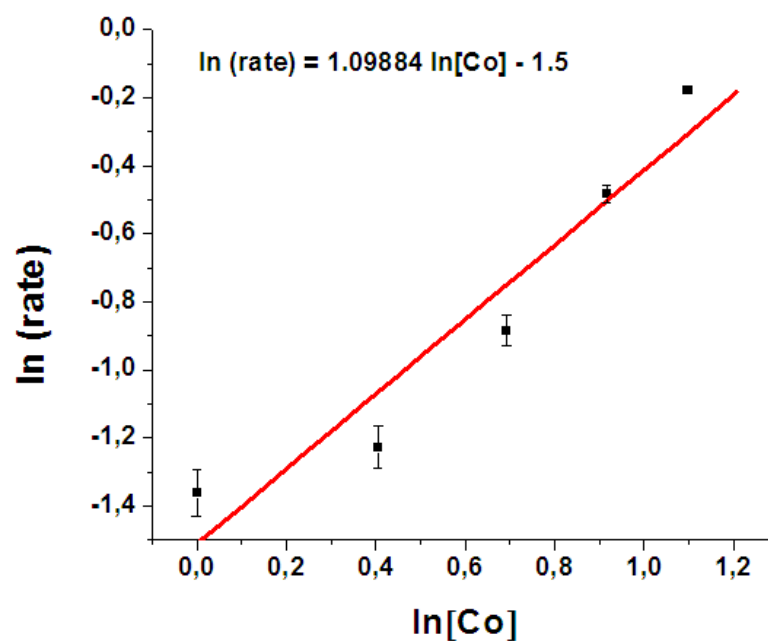


Figure 5.16. The graph of \ln Rate versus \ln [Co] at 25 °C and 150 mM NaBH_4 in the presence of poly(acrylic acid)-stabilizer

The effect of NaBH_4 substrate concentration on the hydrogenation rate was also studied by performing a series of experiments starting with varying initial concentration of NaBH_4 while keeping the catalyst concentration constant at 1.4 mM cobalt(II) chloride in both parts of the experiments. Figure 5.17. and Figure 5.18. show that the rate of reaction does not depend on the NaBH_4 concentration in both two part of the experiments. Plotting $\ln [\text{NaBH}_4]$ vs. \ln rate graph in the presence of hydrogen phosphate-stabilizer and poly(acrylic acid)-stabilizer, where slopes of lines very close to zero, proves that the reaction is zero order with respect to NaBH_4 concentration in both solutions.

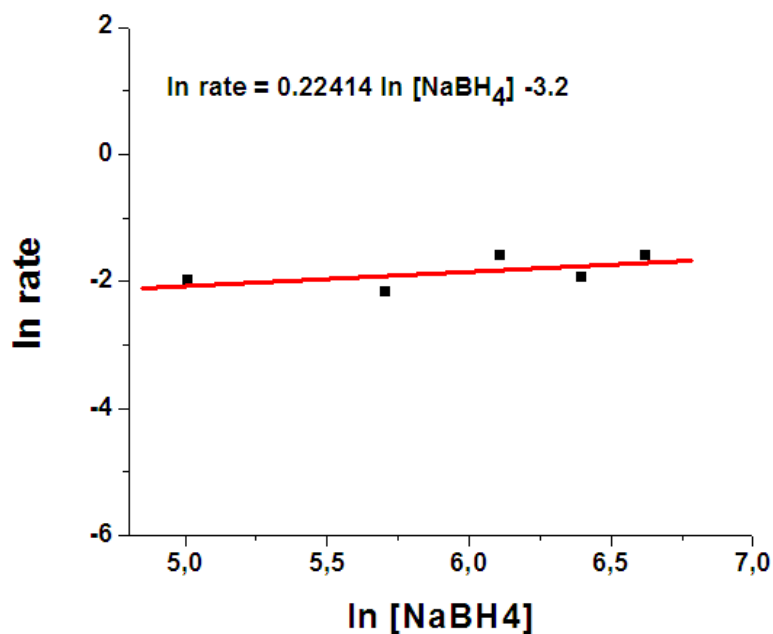


Figure 5.17. The graph of \ln rate versus $\ln [\text{NaBH}_4]$ at constant $[\text{Co}] = 1.4$ mM in the presence of hydrogen phosphate-stabilizer

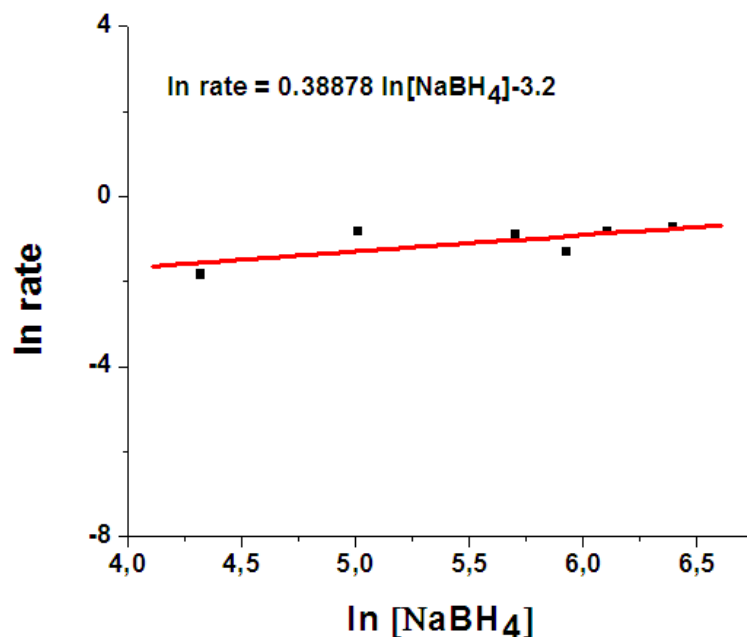


Figure 5.18. The graph of ln rate versus ln [NaBH₄] at constant [Co]=1.4 mM in the presence of poly(acrylic acid)-stabilizer

Thus, the rate law for the catalytic hydrolysis of sodium borohydride can be given as;

$$\frac{-4d[\text{NaBH}_4]}{dt} = \frac{d[\text{H}_2]}{dt} = k [\text{Co}] \quad (2)$$

for both of the solutions.

Cobalt(0) nanoclusters catalyzed and self hydrolysis of sodium borohydride were carried out at various temperature in the range of 20-45 °C starting with the initial substrate concentration of 150 mM NaBH₄ and an initial catalyst concentration of 1.4 mM cobalt(II) chloride. The values of rate constants were calculated from Figure 5.19 and listed in Table 5.1 for the hydrogen phosphate-stabilized Co(0) nanoclusters used as catalyst for the hydrolysis sodium borohydride.

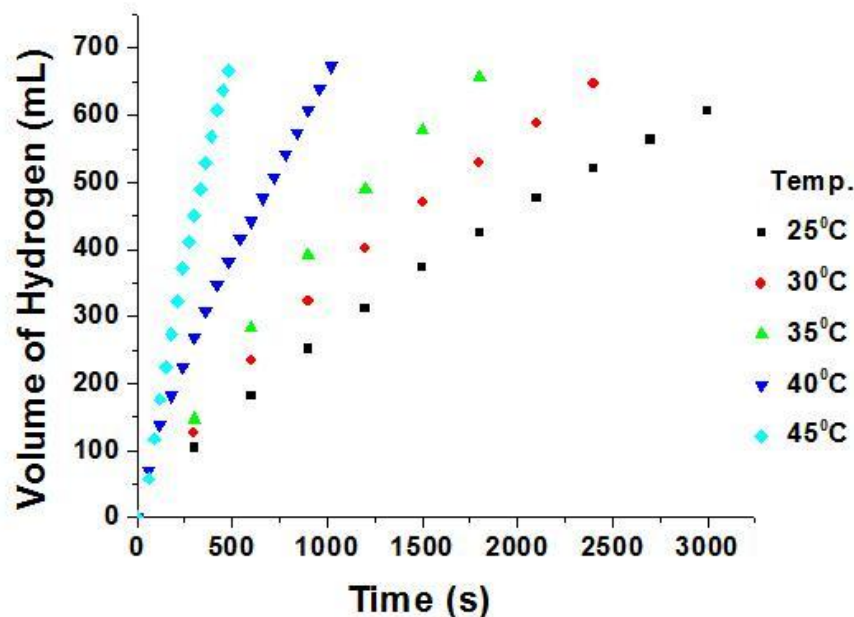


Figure 5.19 The graph of Time(s) vs Volume of hydrogen at different temperatures in all sets $[\text{Co}]=1.4\text{mM}$, $[\text{NaBH}_4]=150\text{mM}$ and $[\text{HPO}_4^{2-}]=4.2\text{mM}$

Table 5.1. Rate constants for the hydrolysis of sodium borohydride catalyzed by Co(0) nanoclusters starting with a solution of 150 mM NaBH₄ and 1.4 mM Cobalt(0) nanoclusters at different temperatures in the presence of hydrogen phosphate as stabilizer.

Temperature (°C)	Rate Constant, k (s ⁻¹)
25	0.115
30	0.164
35	0.228
40	0.346
45	0,451

The rate constant / temperature data was evaluated according to the Arrhenius and Eyring equations to obtain the activation energy, the activation enthalpy and entropy. First, Arrhenius equation was used for the evaluation:

$$k = A e^{\frac{E_a}{RT}} \quad (3)$$

where A and E_a are constant characteristics of the reaction and R is the gas constant. E_a is the Arrhenius activation energy and A is the pre-exponential factor [70]. Taking the natural logarithm of equation (Eq. 3), gives equation (Eq. 4):

$$\ln k = \ln A - \frac{E_a}{RT} \quad (4)$$

Figure 5.20. shows the Arrhenius plot for hydrogen phosphate-stabilized Co(0) nanoclusters, $\ln k$ versus the reciprocal absolute temperature ($1/T$). The slope of straight line gives an activation energy of 53.0 ± 1 kJ/mol for hydrogen phosphate-stabilized cobalt(0) nanoclusters catalyzed hydrolysis of sodium borohydride.

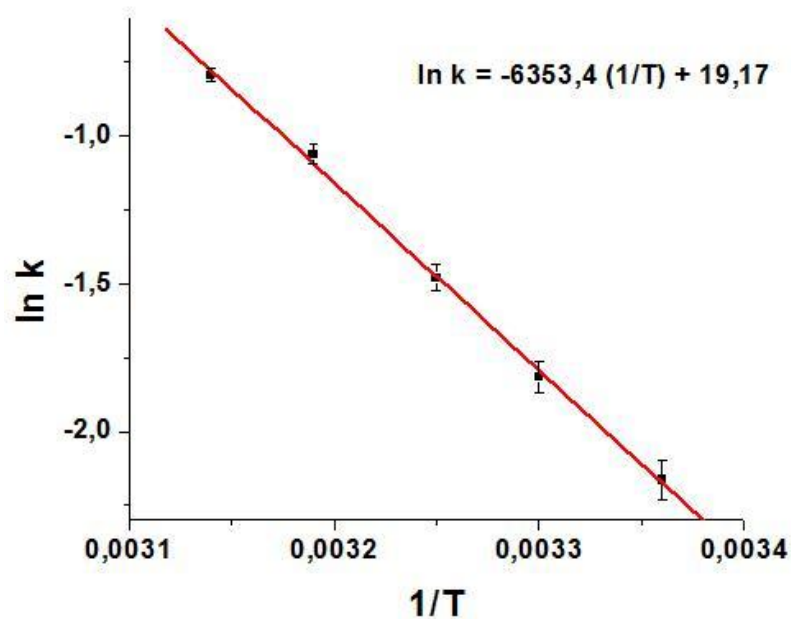


Figure 5.20. The Arrhenius plot, $\ln k$ versus the reciprocal absolute temperature $1/T$, for the hydrolysis of sodium borohydride catalyzed by hydrogenphosphate-stabilized cobalt(0) nanoclusters in the temperature range is 25- 45 °C.

The values of rate constant were calculated from Figure 5.21. and listed in Table 5.2 for the poly(acrylic acid)-stabilized Co(0) nanoclusters used as catalyst for the hydrolysis sodium borohydride.

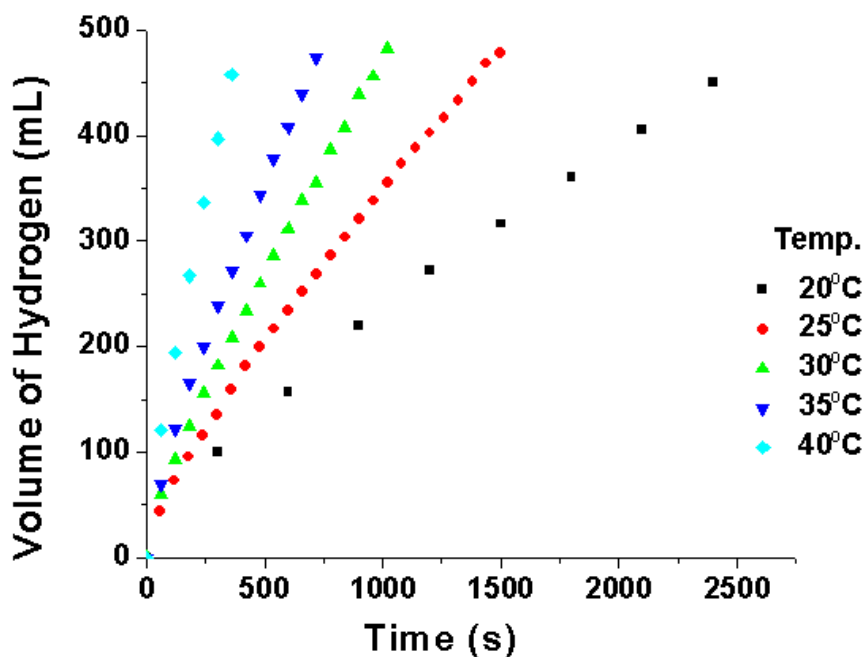


Figure 5.21 The graph of Time(s) vs Volume of hydrogen at different temperatures in all sets $[Co]=1.4mM$, $[NaBH_4]=150mM$ and $[PAA]=4.2mM$

Table 5.2. Rate constants for the hydrolysis of sodium borohydride catalyzed by Co(0) nanoclusters starting with a solution of 150 mM NaBH₄ and 1.4 mM Cobalt(0) nanoclusters at different temperatures in the presence of poly(acrylic acid) as stabilizer.

Temperature (°C)	Rate Constant, k (s ⁻¹)
20	0,122
25	0,185
30	0,273
35	0,369
40	0,595

Figure 5.22. shows Arrhenius plot for poly(acrylic acid) stabilized Co(0) nanoclusters, $\ln k$ versus the reciprocal absolute temperature ($1/T$). The slope of

straight line gives an activation energy of 58.8 ± 1 kJ/mol for cobalt(0) nanoclusters catalyzed hydrolysis of sodium borohydride.

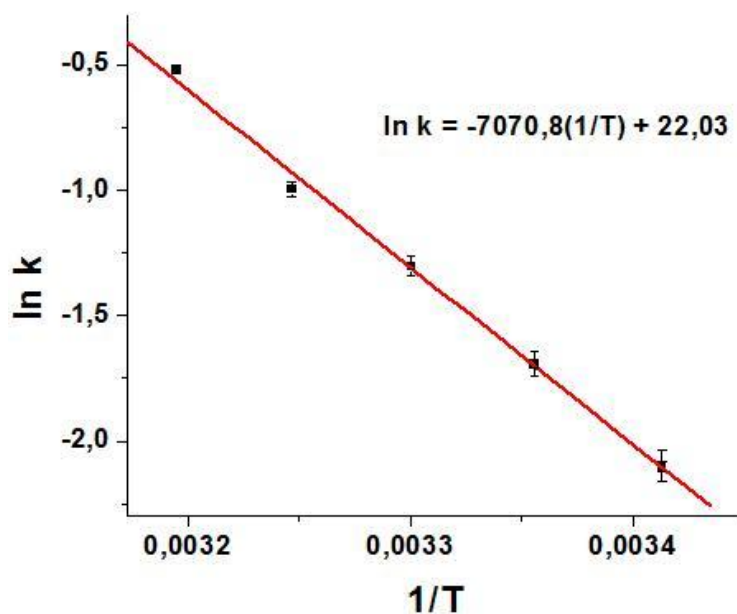


Figure 5.22. The Arrhenius plot, $\ln k$ versus the reciprocal absolute temperature $1/T$, for the hydrolysis of sodium borohydride catalyzed by poly(acrylic acid)-stabilized cobalt(0) nanoclusters in the temperature range is 20- 40 °C.

Activation energies for the hydrolysis of sodium borohydride catalyzed by hydrogenphosphate-stabilized Co(0) nanoclusters, poly(acrylic acid)-stabilized cobalt(0) nanoclusters and other catalysts are listed in Table 5.3 for comparison.

Table 5.3. Arrhenius activation energy for various catalyst systems used for the hydrolysis of sodium borohydride

Catalyst	Activation Energy (kJ mol ⁻¹)
HPO ₄ ²⁻ -stabilized Co(0) nanoclusters	53
Poly(acrylic acid)-stabilized Co(0) nanoclusters	58.8
Poly(N-vinyl-2-pyrrolidone)-stabilized Ni(0) nanoclusters [71]	48
HPO ₄ ²⁻ -stabilized Ni(0) nanoclusters [28]	54
Ru(0) nanoclusters [21]	42
Bulk nickel [11]	71
Bulk cobalt [11]	75

The enthalpy of activation, ΔH^\ddagger and the entropy of activation, ΔS^\ddagger were calculated according to the Eyring equation [72] (**Eq. 5**) by drawing the graph of $\ln \frac{k}{T}$ versus $\frac{1}{T}$,

$$\ln \frac{k}{T} = \frac{1}{T} \left(\frac{\Delta H^\ddagger}{R} \right) + \ln \frac{k_b}{h} + \frac{\Delta S^\ddagger}{R} \quad (5)$$

where “ k_b ” is Boltzmann's constant ($1.381 \cdot 10^{-23} \text{ J} \cdot \text{K}^{-1}$), “ h ” is Plank constant ($6.626 \cdot 10^{-34} \text{ J} \cdot \text{s}$).

Figure 5.23. shows the Eyring plot, $\ln (k/T)$ versus reciprocal absolute temperature ($1/T$) for hydrogen phosphate stabilized Co(0) nanoclusters. The slope of straight line gives an activation enthalpy of $52.8 \pm 1 \text{ kJ/mol}$ and extrapolation of straight line gives activation entropy of $-86.0 \pm 3 \text{ J/(mol.K)}^{-1}$.

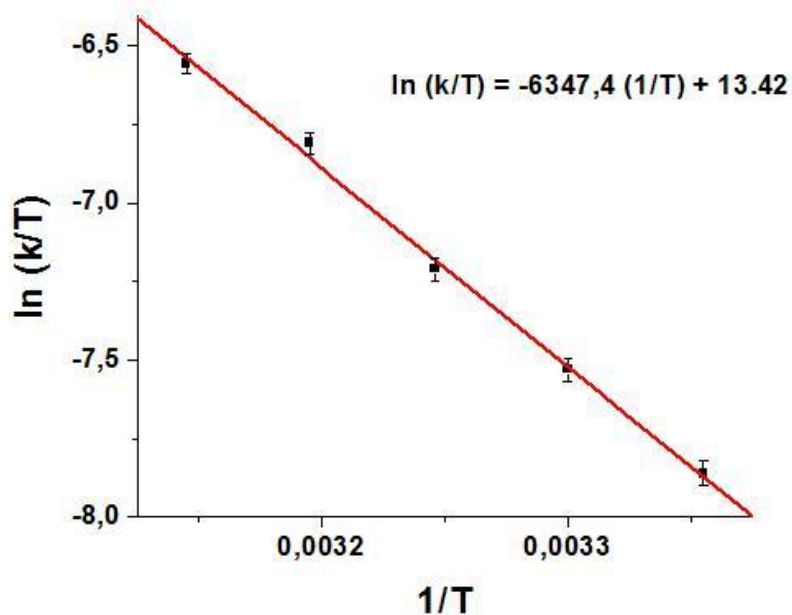


Figure 5.23. The Eyring plot, $\ln (k/T)$ versus the reciprocal absolute temperature $1/T$, for the hydrolysis of sodium borohydride catalyzed by hydrogenphosphate-stabilized cobalt(0) nanoclusters in the temperature range 25-45 °C

Figure 5.24. shows the Eyring plot, $\ln (k/T)$ versus reciprocal absolute temperature ($1/T$) for poly(acrylic acid)-stabilized Co(0) nanoclusters. The slope of straight line gives an activation enthalpy of 56.5 ± 1 kJ/mol and extrapolation of straight line gives activation entropy of -69.5 ± 3 J/(mol.K)⁻¹.

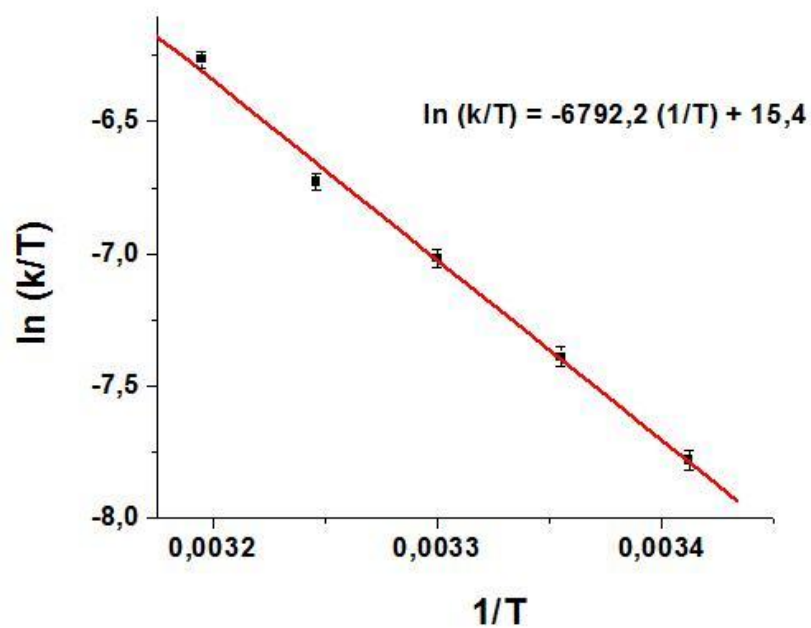


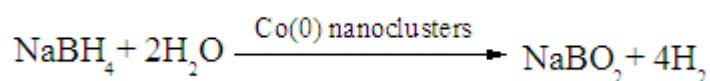
Figure 5.24. The Eyring plot, $\ln(k/T)$ versus the reciprocal absolute temperature $1/T$, for the hydrolysis of sodium borohydride catalyzed by poly(acrylic acid)-stabilized cobalt(0) nanoclusters in the temperature range 20-40 °C

CHAPTER 6

CONCLUSIONS

In summary, our study on the effect of stabilizer on the catalytic activity of cobalt(0) nanoclusters as catalyst for the hydrolysis of sodium borohydride have led to the following conclusions and insights;

- Cobalt(0) nanoclusters can be prepared in-situ during the hydrolysis of sodium borohydride from reduction of a commercially available precursor material and stabilized by hydrogenphosphate anion or poly(acrylic acid) in aqueous solution.
- Hydrogenphosphate anion is a good electrostatic stabilizer for cobalt(0) nanoclusters because of excellent size matching between O-O distance (2.52 Å) of hydrogenphosphate and cobalt-cobalt distance (2.50 Å) on the nanocluster surface. On the other hand, poly(acrylic acid) is a good steric stabilizer for cobalt(0) nanoclusters showing the best catalytic activity among the lots of polymers.
- Water-dispersible hydrogenphosphate-stabilized and poly(acrylic acid)-stabilized cobalt(0) nanoclusters are both highly active catalysts in the hydrolysis of sodium borohydride even at room temperature.



- Sodium borohydride can be used as hydrogen storage material since it provides a safe and practical mean of producing hydrogen at ambient temperature, when water dispersible hydrogenphosphate-stabilized and poly(acrylic acid)-stabilized cobalt(0) nanoclusters are used as catalyst.
- The rate law of the hydrolysis of sodium borohydride catalyzed by the hydrogenphosphate-stabilized and poly(acrylic acid)-stabilized cobalt(0) nanoclusters can be given as;

$$\frac{-4d[\text{NaBH}_4]}{dt} = \frac{d[\text{H}_2]}{dt} = k [\text{Co}]$$

The catalytic hydrolysis of sodium borohydride is first order with respect to the catalyst concentration and zero order with respect to the substrate concentration in the case of both stabilizers hydrogen phosphate and poly(acrylic acid).

- The activation energy (E_a), activation enthalpy (ΔH^\ddagger) and activation entropy (ΔS^\ddagger) of hydrogen phosphate stabilized cobalt(0) nanoclusters catalyzed hydrolysis of sodium borohydride were found to be 53.0 ± 1 kJ/mol, 52.8 ± 1 kJ/mol and -86.0 ± 3 J/(mol.K)⁻¹. On the other hand, those values were found to be 58.8 ± 1 kJ/mol, 56.5 ± 1 kJ/mol and -69.5 ± 3 J/(mol.K)⁻¹ for poly(acrylic acid) stabilized cobalt(0) nanoclusters, respectively.
- The lifetime of cobalt(0) nanoclusters catalyst depends on the nature of stabilizer used. Hydrogen phosphate-stabilized Co(0) nanoclusters are highly active catalyst providing 1285 total turnovers in the hydrolysis of sodium borohydride over 4 hours before they are deactivated and the recorded turnover frequency (TOF) is 5.35 min⁻¹. On the other hand, poly(acrylic acid)-stabilized Co(0) nanoclusters are highly active catalyst, also with long

lifetime providing 6600 total turnovers over 36 hours before they are deactivated with a turnover frequency of 3.05 min^{-1} .

REFERENCES

- [1] Zerta M., Schmidt P.R., Stiller C., Landinger H., *Int. J. Hydrogen Energy*, **2008**, 33, 3021-3025.
- [2] Veziroğlu T.N., Şahin S., *Energy Conversion and Management*, **2008**, 49, 1820–1831.
- [3] Jean-Baptiste P., Ducroux R., *Energy Policy*, **2003**, 31, 155–166.
- [4] Vriese B.J.M., Vuuren D.P., Hoogwijk M.M., *Energy Policy*, **2007**, 35, 2590–2610.
- [5] Basic Research Needs For the Hydrogen Economy, Report of the Basic Energy Sciences Workshop on Hydrogen Production, Storage and Use, May 13-15, **2003**, Office of Science, U. S. Department of Energy, www.sc.doe.gov/bes/hydrogen.pdf, last visited on December 2009
- [6] Lattina W.C., Utgikarb V.P., *International Journal of Hydrogen Energy*, **2007**, 32, 3230 – 3237.
- [7] Holladay J.D., Hu J., King D.L., Wang Y., *Catalysis Today*, **2009**, 139, 244 -260.
- [8] Felderhoff M., Weidenthaler C., Helmoltb R.V., Eberleb U., *Phys. Chem. Chem. Phys.*, **2007**, 9, 2643–2653.
- [9] Amendola S.C., Stefanie L., Goldman S., Janjua M. S., Kelly M.T., Petillo P.J., Binder M., *J. Power Sources*, **2000**, 85, 186–189.
- [10] (a) Wang P., Kang X., *Dalton Trans.*, **2008**, 40, 5400-5413. (b) Deng Z.Y., Ferreira J.M.F., Sakka Y., *J. Am. Ceram. Soc.*, **2008**, 91(12), 3825–3834. (c) Wang H.Z., Leung D.Y.C., Leung M.K.H., Ni M., *Renewable and Sustainable Energy Reviews*, **2009**, 13, 845-85. (d) Amendola S.C., Sharp-Goldman S.L., Janjua M.S., Spencer N.C., Kelly M.T., Petillo P.J., Binder M., *Int. Journal of Hydrogen Energy*, **2000**, 25, 969-975. (e) Sherif S.A., Barbir F., Veziroglu T.N., *Solar Energy*, **2005**, 78, 647-660.
- [11] (a) Levy A., Brown J.B., Lyons C.J., *Ind. Eng. Chem.*, **1960**, 52, 211. (b) Kaufman C.M., Sen B., *J. Chem. Soc. Dalton Trans.*, **1985**, 307. (c) Brown H.C., C.A. Brown, *J. Am. Chem. Soc.*, **1962**, 84, 1493.

- [12] Schlesinger H.I., Brown H.C., Finholt A.B., Gilbreath J.R., Hockstra H.R., Hydo E.K., *J. Am. Chem. Soc.*, **1953**, 75, 215.
- [13] Levy A., Brown J.B., Lyons C.J., *Ind. Eng. Chem.*, **1960**, 52, 211.
- [14] Brown H.C., Brown C.A., *J. Am. Chem. Soc.*, **1962**, 84, 1493.
- [15] Kaufman C.M., Sen B., *J. Chem. Soc. Dalton. Trans.*, **1985**, 83, 307.
- [16] Korobov I.I., Mozhina N.G., Blinova L.N., *Kinet. Catal.*, **1995**, 48, 380.
- [17] Amendola S.C., Onnerud P., Kelly M.T., Petillo P.J., Sharp-Goldman S.L., Binder M., *J. Power Sources*, **2000**, 85, 186.
- [18] Kojima Y., Suzuki K.I., Fukumoto K., Sasaki M., Yamamoto T., Kawai Y., Hayashi H., *Int. J. Hydr. Energy*, **2002**, 27, 1029.
- [19] Hua D., Hanxi Y., Xinping A., Chuansain C., *Int. J. Hydr. Energy*, **2003**, 28, 1095.
- [20] Kim J.H., Lee H., Han S.C., Kim H.S., Song M.S., Lee J.Y., *Int. J. Hydr. Energy*, **2004**, 29, 263.
- [21] Zahmakıran M., Özkar S., *Journal of Molecular Catalysis A: Chemical*, **2006**, 258, 95–103.
- [22] Özkar S., Zahmakıran M., *Journal of Alloys and Compounds*, **2005**, 404–406, 728–731.
- [23] Ott L.S., Finke R.G., *Coordination Chemistry Reviews*, **2007**, 251, 1075–1100.
- [24] (a) Turkevich J., Kim G., Hillier J., *Discuss. Faraday Soc.*, **1951**, 11, 55-75 (b) Hirai H., Nakao Y., Toshima N., Adachi K., *Chem. Lett.*, **1976**, 5, 905-910. (c) Giersig M., Mulvaney P., *Langmuir*, **1993**, 9 (12), 3408-3413. (d) Kaupp M., Wllen C. V., Franke R., Schmitz F., Kutzelnigg W., *J. Am. Chem. Soc.*, **1996**, 118 (47), 11939-11950.
- [25] Turkevich J., Kim G., Hillier J., *Discuss. Faraday Soc.*, **1951**, 11, 55-75.
- [26] Hirai H., Nakao Y., Toshima N., Adachi K., *Chem. Lett.*, **1976**, 5, 905-910.
- [27] Finke R.G., Özkar S., *Coordination Chemistry Reviews*, **2004**, 248, 135-146.
- [28] Metin Ö., Özkar S., *International Journal of Hydrogen Energy*, **2007**, 32, 1707–1715.
- [29] Özkar S., Finke R. G., *Langmuir*, **2003**, 19, 6247-6260.

- [30] Gagnon L., Energy Policy, **2008**, 36, 3317– 3322.
- [31] Zerta M., Schmidt P.R., Stiller C., Landinger H., International Journal of Hydrogen Energy, **2008**, 33, 3021 – 3025.
- [32] Jean-Baptistea P., Ducroux R., Energy Policy, **2003**, 31, 155–166.
- [33] Penner S.S., Energy, **2006**, 31, 33–43.
- [34] Kotay S.M., Das D., International Journal of Hydrogen Energy, **2008**, 33(1):258–263.
- [35] U.S. Department of Energy. Office of fossil energy—Hydrogen Program Plan: Hydrogen from Natural Gas and Coal: the Road to a Sustainable Energy Future. Available at <http://fossil.energy.gov/programs/fuels/publications/programplans/2003/fehydrogenplan2003.pdf>, last visited on December 2009
- [36] Ni M., Leung M.K.H., Leung D.Y.C., Sumathy K., Renewable Sustainable Energy Rev. **2007**, 11, 401–425.
- [37] Ni M., Leung D.Y.C., Leung M.K.H., Fuel Process Technology, **2006**, 87, 461–472.
- [38] Wang H.Z., Leung D.Y.C., Leung M.K.H., Ni M., Renewable and Sustainable Energy Reviews, **2009**, 13, 845–853.
- [39] Pozioa A., Francescoa M.D., Monteleonea G., Oronzioa R., Gallia S., D’Angelob C., Marruccib M., International Journal of Hydrogen Energy, **2008**, 33, 51 – 56.
- [40] Yukawa H., Matsumura T., Morinaga M., Journal of Alloys and Compounds, **1999**, 293–295, 227–230.
- [41] Ingersoll J.C., Mania N., Thenmozhiyal J.C., Muthaiah A., Journal of Power Sources, **2007**, 173, 450–457.
- [42] Cho K.W., Kwon H.S., Catalysis Today, **2007**, 120, 298–304.
- [43] Amendola S.C., Sharp-Goldman S.L., Janjua M.S., Spencer N.C., Kelly M.T., Petillo P.J., Binder M., International Journal of Hydrogen Energy, **2000**, 25, 969–975.
- [44] Liu B.H., Li Z.P., Journal of Power Sources, **2009**, 187, 527–534.

- [45] Aiken III J.D., Finke R.G., *Journal of Molecular Catalysis A: Chemical*, **1999**, 145, 1–44.
- [46] Özkaz S., Finke R.G., *Langmuir*, **2003**, 19, 6247-6260.
- [47] Ott L.S., Finke R.G., *Inorg. Chem.*, **2006**, 45, 8382-8393.
- [48] (a) Fu X., Wang Y., Wu N., Gui L., *Langmuir*, **2002**, 18, 4619 (b) Toshima N., Wang Y., *Chem. Lett.*, **1993**, 22, 1611 (c) Henglein A., Holzwarth A., Mulvaney P., *J. Phys. Chem.*, **1992**, 96,8700 (d) Ershov B.G., Janata E., Michaelis M., Henglein A., *J. Phys. Chem.*, **1991**, 95, 8996 (e) Suslick K.S., Prince J., *Annu. Rev. Mater. Sci.*, **1999**, 29, 295.
- [49] Lin Y., Finke R.G., *J. Am. Chem. Soc.*, **1994**, 116, 8335-8353.
- [50] Reetz M.T., Breinbauer R., Wedemann P., Binger P., *Tetrahedron*, **1998**, 54, 1233-1240.
- [51] Lewis L.N., Lewis N., *J. Am. Chem. Soc.*, **1986**, 108, 7228-7231.
- [52] Wilcoxon J.P., Martino T., Klavetter E., Sylwester A.P., *Nanophase Mater.*, **1994**, 771-780.
- [53] Schmidt T.J., Noeske M., Gasteiger H.A., Behm R.J., Britz P., Brijoux W., Bönnemann H., *Langmuir*, **1997**, 13, 2591.
- [54] Vargaftik M.N., Zargorodnikov V.P., Stolarov I.P., Moiseev I.I., Kochubey D.I., Likholobov V.A., Chuvilin A.L., Zamaraev K.I., *J. Mol. Catal.*, **1989**, 53, 315-348.
- [55] Reetz M.T., Quaiser S.A., Merk C., *Chem. Ber.*, **1996**, 129, 741-743.
- [56] Reetz M.T., Breinbauer R., Wanninger K., *Tetrahedron Lett.*, **1996**, 37, 4499-4502.
- [57] Reetz M.T., Lohmer G., *J. Chem. Soc., Chem. Commun.*, **1996**, 1921-1922.
- [58] Bönnemann H., Braun G.A., *Angew Chem., Int. Ed. Engl.*, **1996**, 35, 1992.
- [59] Hornstein B.J., Finke R.G., *Chem. Mater.* **2004**, 16, 139-150.
- [60] Ninham B. W., *Adv. Colloid Interface Sci.*, **1999**, 83, 1-17.
- [61] Roucoux A., Schulz J., Patin H., *Chem. Rev.*, **2002**, 102, 3757-3778.
- [62] Widegren J.A., Finke R.G., *Journal of Molecular Catalysis A: Chemical*, **2003**, 191, 187–207.

- [63] Toshima N., Harada M., Yonezawa T., Kushihashi K., Asakura K., *J. Phys. Chem.*, **1991**, 95 (19), 7448-7453.
- [64] Willner I., Mandler D.J., *J. Am. Chem. Soc.*, **1989**, 111, 1330.
- [65] Corain B., Schmid G., Toshima N., *Metal Nanoclusters in Catalysis and Materials Science* 1st edition, Elsevier B.V., **2008**.
- [66] Watzky M. A., Finke R. G., *J. Am. Chem. Soc.*, **1997**, 119, 10382-10400.
- [67] Tan B. J., Klabunde J. K., Sherwood P. M. A., *J. Am. Chem. Soc.* 1991, 113, 855-861
- [68] Gleason N. R. and Zaera F., *J. Catal.*, **1997**, 169 365
- [69] H.I. Schlesinger, H.C. Brown, A.E. Finholt, J.R. Gilbreath, H.R. Hoekstra, E.K.Hyde, *J. Am. Chem. Soc.*, **1953**,75,215.
- [70] R.J. Silbey, R.A. Alberty, *Physical Chemistry*, 3rd edition ; John Wiley&Sons, Inc., **2001**.
- [71] Metin Ö., Özkar S., *Journal of Molecular Catalysis A: Chemical*, **2008**, 295, 39-46
- [72] Wilkins R. G., *Kinetics and Mechanism of Reactions of Transition Metal Complexes*, 2nd edition ; VCH Publishers, Inc., New York, **1991**.

APPENDIX A

The kinetic data of the hydrogenphosphate-stabilized and polyacrylic acid-stabilized cobalt(0) nanoclusters catalyzed hydrolysis of sodium borohydride studied by monitoring the hydrogen evolution depending on substrate concentration, catalyst concentration, stabilizer concentration and temperature.

Table A.1. Volume of hydrogen generated versus time for hydrogenphosphate-stabilized cobalt(0) nanoclusters catalyzed hydrolysis of sodium borohydride at different cobalt(II)chloride concentrations.

[NaBH₄]=150mM, 25±0.1⁰C

Time (s)	1.0mM	1.2mM	1.4mM	1.6mM	1.8mM	2.0mM
300	69.36	86.7	104.04	121.38	138.72	156.06
600	121.38	156.06	182.07	208.08	242.76	277.44
900	173.4	216.75	251.43	277.44	329.46	372.81
1200	216.75	277.44	312.12	338.13	398.82	459.51
1500	260.1	329.46	372.81	398.82	468.18	546.21
1800	294.78	381.48	424.83	459.51	537.54	632.91
2100	329.46	424.83	476.85	520.2	606.9	689.61
2400	364.14	468.18	520.2	572.22	672	
2700	398.82	511.53	563.55	624.24		
3000	433.5	546.21	606.9	672		
3300	468.18	580.89	650.25			
3600	502.86	615.57				
3900	537.54					
4200	572.22					

Table A.2. Volume of hydrogen generated versus time for polyacrylic acid - stabilized cobalt(0) nanoclusters catalyzed hydrolysis of sodium borohydride at different cobalt(II)chloride concentrations.

[NaBH₄]=150mM, 25±0.1⁰C

Time (s)	1.0mM	1.5mM	2.0mM	2.5mM	3.0mM	3.5mM
60	52.02	64.16	60.69	86.7	112.71	112.71
120	78.03	100.57	104.04	138.72	173.4	171.67
180	95.37	124.85	130.05	185.84	235.82	221.95
240	116.18	150.86	162.99	227.15	287.84	268.77
300	136.93	175.13	189.01	258.37	343.33	324.26
360	149.124	192.47	220.22	301.72	378.01	364.14
420	169.93	206.35	247.96	336.39	424.83	416.16
480	185.54	228.89	270.5	371.08	476.85	
540	202.88	241.03	294.78	398.82		
600	218.48	260.1	317.32	426.56		
660	234.09	277.44	345.07			
720	244.49	294.78	369.35			
780	261.83	308.65	390.15			
840	279.17	324.26	410.97			
900	291.31	338.13	436.98			
960	308.65	350.27				
1020	320.79	362.41				
1080	338.13	374.54				
1140	353.74					

Table A.3. Volume of hydrogen generated versus time for hydrogenphosphate-stabilized cobalt(0) nanoclusters catalyzed hydrolysis of sodium borohydride in different NaBH₄ concentrations.

[CoCl₂.6H₂O]=1.4mM, 25±0.1⁰C

e

Time(s)	150mM	300mM	Time(s)	450mM	Time(s)	600mM	750mM
300	66.12	69.36	120	59.16	300	78.03	112.71
600	107.88	121.38	240	100.92	600	147.39	182.07
900	149.64	164.73	360	146.16	900	208.08	242.76
1200	201.84	216.75	480	189.66	1200	251.43	303.45
1500	245.34	251.43	600	224.46	1500	294.78	355.47
1800	285.36	286.11	720	259.26	1800	338.13	407.49
2100	321.9	320.79	840	288.84	2100	381.48	450.84
2400	354.96	341.598	960	316.68	2400	416.16	494.19
2700		376.278	1080	341.04	2700	459.51	
3000		397.086	1200	365.4	3000	485.52	
3300		419.628	1320	389.76			
3600		433.5	1440	412.38			

Table A.4. Volume of hydrogen generated versus time for polyacrylic acid-stabilized cobalt(0) nanoclusters catalyzed hydrolysis of sodium borohydride in different NaBH₄ concentrations.

[CoCl₂.6H₂O]=1.4mM, 25±0.1⁰C

Time (s)	75.0m M	Time (s)	150.0m M	300.0m M	375.0m M	450.0m M	600.0m M
120	69.6	60	42	69.36	57.81	86.7	83.23
240	104.4	120	72	104.04	83.19	130.05	126.58
360	139.2	180	102	130.05	108.57	164.73	161.26
480	161.82	240	124.5	156.06	131.13	194.21	192.47
600	186.18	300	154.5	185.54	155.1	225.42	221.95
720	210.54	360	178.5	213.28	170.61	251.43	247.96
840	229.68	420	204	234.09	195.99	286.11	282.64
960	252.3	480	237	254.89	215.73	312.12	308.65
1080	271.44	540	259.5	275.71	229.83	338.13	338.13
1200	288.84	600	289.5	299.98	246.75	364.14	369.34
1320	309.72	660	315	325.99	263.67	390.15	395.35
1440		720	336	348.53	279.18	416.16	421.36
		780	361.5	365.87	294.69	442.17	447.37
		840	384	388.42	310.2	468.18	473.38
				409.22	328.53		
				426.56	338.4		
				449.11	352.5		
				468.18	366.6		
					380.4		

Table A.5. Volume of hydrogen(mL) versus time (s) in hydrogen phosphate-stabilized cobalt(0) nanoclusters catalyzed hydrolysis of sodium borohydride at constant $\text{CoCl}_2 \cdot 6\text{H}_2\text{O}$ and NaBH_4 concentrations, $[\text{CoCl}_2 \cdot 6\text{H}_2\text{O}] = 1.4\text{mM}$, $[\text{NaBH}_4] = 150\text{mM}$, at different temperatures (25°C - 45°C)

Time	25°C	Time	30°C	Time	35°C	Time	40°C	Time	45°C
300	104,04	300	127,4	300	147	60	69,36	60	58,8
600	182,07	600	235,2	600	284,2	120	138,72	90	117,6
900	251,43	900	323,4	900	392	180	182,07	120	176,4
1200	312,12	1200	401,8	1200	490	240	225,42	150	225,4
1500	372,81	1500	470,4	1500	578,2	300	268,77	180	274,4
1800	424,83	1800	529,2	1800	656,6	360	307,785	210	323,4
2100	476,85	2100	588			420	346,8	240	372,4
2400	520,2	2400	646,8			480	381,48	270	411,6
2700	563,55					540	416,16	300	450,8
3000	606,9					600	442,17	330	490
						660	476,85	360	529,2
						720	508,062	390	568,4
						780	541,586	420	607,6
						840	574,532	450	637
						900	607,478	480	666,4
						960	640,424		
						1020	673,37		

Table A.6. Volume of hydrogen(mL) versus time (s) in polyacrylic acid-stabilized cobalt(0) nanoclusters catalyzed hydrolysis of sodium borohydride at constant $\text{CoCl}_2 \cdot 6\text{H}_2\text{O}$ and NaBH_4 concentrations, $[\text{CoCl}_2 \cdot 6\text{H}_2\text{O}] = 1.4\text{mM}$, $[\text{NaBH}_4] = 150\text{mM}$, at different temperatures (20°C - 40°C)

Time	20 ⁰ C	Time	25 ⁰ C	Time	30 ⁰ C	Time	40 ⁰ C	Time	45 ⁰ C
600	157,41	120	72,83	120	93,64	120	121,38	120	194,208
900	219,78	180	95,37	180	124,85	180	164,73	180	267,036
1200	271,755	240	116,18	240	156,06	240	199,41	240	336,396
1500	316,305	300	135,25	300	182,07	300	239,23	300	397,086
1800	360,855	360	159,53	360	208,8	360	272,24	360	457,776
2100	405,405	420	182,07	420	234,1	420	305,18		
2400	449,955	480	199,41	480	260,1	480	343,33		
		540	216,75	540	286,11	540	378,01		
		600	234,09	600	312,12	600	407,49		
		660	251,43	660	338,13	660	438,7		
		720	268,77	720	355,47	720	473,38		
		780	286,11	780	386,68				
		840	303,45	840	407,49				
		900	320,79	900	438,7				
		960	338,13	960	456,04				
		1020	355,47	1020	482,05				
		1080	372,81						
		1140	388,42						
		1200	402,29						
		1260	416,16						
		1320	433,5						
		1380	450,84						
		1440	468,18						
		1500	478,58						